Updated 3D basin model and NZS 1170.5 subsoil class and site period maps for the Wellington CBD: Project 2017-GNS-03-NHRP

AE Kaiser
S Bourguignon
S Giallini
MP Hill
ZR Bruce
L Wotherspoon
R Morgenstern

GNS Science Consultancy Report 2019/01
May 2019

GNS SCIENCE
TE PŪ AO

DISCLAIMER

This report has been prepared by the Institute of Geological and Nuclear Sciences Limited (GNS Science) exclusively for and under contract to Natural Hazards Research Platform. Unless otherwise agreed in writing by GNS Science, GNS Science accepts no responsibility for any use of or reliance on any contents of this report by any person other than Natural Hazards Research Platform and shall not be liable to any person other than Natural Hazards Research Platform, on any ground, for any loss, damage or expense arising from such use or reliance.

Use of Data:

Date that GNS Science can use associated data: January 2019

BIBLIOGRAPHIC REFERENCE

Kaiser AE, Hill MP, Wotherspoon L, Bourguignon S, Bruce ZR, Morgenstern R, Giallini S. 2019. Updated 3D basin model and NZS 1170.5 subsoil class and site period maps for the Wellington CBD: Project 2017-GNS-03-NHRP. Lower Hutt (NZ): GNS Science. 48 p. + appendix. Consultancy Report 2019/01.

CONTENTS

FIGURES

TABLES

APPENDICES

EXECUTIVE SUMMARY

Soil deposits in sedimentary basins are well-known for amplifying earthquake ground motion. Models of the 3D subsurface and maps of key geotechnical parameters are important to mitigate these effects and guide robust engineering design practices. Furthermore, they can help us better understand ground motion amplification and damage patterns observed in recent earthquakes in Wellington.

Following the 2016 Mw 7.8 Kaikōura earthquake, we have updated the central Wellington 3D basin model and low amplitude natural site period and NZS 1170.5 site subsoil class maps for central Wellington. The new maps incorporate significant new geotechnical and geophysical data collected since the original work of Semmens *et al.* (2010), including 700+ new boreholes records collated from a range of sources and 400+ new geophysical measurements collected as part of this project.

We have compiled an upgraded borehole database comprising 1,427 boreholes, 429 of which intersect greywacke basement. The database allows us to better define key geotechnical engineering units within our 3D model, in particular shallow loose sediments and areas of hydraulic and engineered fill in the uppermost 30 m. The surface geology map has also been updated based on boreholes, aerial photography and LiDAR digital terrain models. The result is a new (v2.0) 3D geological and velocity model for central Wellington.

We have also compiled a new geophysical site period database from microtremor horizontal-to-vertical spectral ratio (HVSR) surveys. The database includes an estimate of quality for each individual site period measurement. The geophysical information complements the borehole information by providing key constraints on site period and basin structure in deeper parts of the basin where boreholes to basement are sparse.

Finally, we draw together the large quantity of complementary geological and geophysical information in an innovative scheme to provide updated maps of natural site period and site subsoil class. Our results indicate that site period is longer than previously thought in the upper Thorndon basin. This implies that the depth to greywacke basement is likely deeper than previously mapped, and site Class D is the most appropriate NZS1170.5 subsoil classification. Furthermore, the variability of site period estimates in the Thorndon area, indicates that complex amplification effects are present, likely associated with the Wellington Fault basin edge and lateral 3D subsurface variations. In waterfront areas, including CentrePort, site period is mapped in the 1–2 s period range corresponding to that of large amplifications observed during the Kaikōura earthquake. Further acquisition of deep boreholes intersecting basement in the Thorndon and CentrePort area and on the footwall adjacent to the Wellington fault, would provide valuable confirmation of the deeper basin structure in this area.

The Te Aro basin to the south is now mapped with more steeply dipping basement on its western and eastern flanks. This is consistent with the new discovery of Aotea Fault offshore, which is inferred to extend beneath the eastern edge of the basin. Geological and geophysical estimates of site period in the Te Aro basin are generally in excellent agreement and allow well-constrained and smoothly varying site period contours to be mapped. Our study highlights that areas above the steeply-sided basin edges adjacent to deep soils may experience longer period site response than implied by considering only the 1D profile beneath the site.

1.0 INTRODUCTION

The character and spatial extent of local ground motion amplification depends on the geological structure and local geotechnical soil properties. In sedimentary basins, seismic waves are amplified and/or trapped within softer materials with lower shear-wave velocity (Vs) and lower density that are encountered at shallow depths near the surface. The period at which this amplification occurs is related primarily to the Vs and thickness properties of the subsoil. Amplification can also be enhanced by basin effects arising from 3D basin structure, including potential 'basin-edge generated waves' arising from the sharp rock-to-soil material contrasts at the steep-sided basin margins. Hence, detailed knowledge of the subsurface is necessary to guide earthquake-resistant design and mitigate the effects of large damaging earthquakes.

The central business district (CBD) of Wellington, New Zealand's capital city, overlies the edge of the Wellington sedimentary basin (Figure 1.1). The underlying subsurface basement topography includes strong lateral variations and steeply dipping basin edges (Semmens *et al.* 2010), making the city prone to complex, spatially variable amplification effects. Furthermore, it is located in a region of high seismic hazard. Several faults located within ~50 km of the city are capable of generating M7.5+ earthquakes, including the Wellington Fault, and the underlying Hikurangi subduction interface (Stirling *et al.* 2012).

Most recently, the November 2016 Mw 7.8 Kaikōura earthquake rupture terminated ~60 km from the central city, causing significant disruption and damage. The observed damage was concentrated in mid-rise structures (5 to 15 storeys) and was clearly exacerbated by the presence of basin amplification at a period of 1–2 seconds, corresponding to the typical fundamental period of these types of structures (Kaiser *et al.* 2017a; Bradley *et al.* 2017, 2018). Spectral accelerations were systematically amplified in the 1–2 s period range across all 'deep or soft soil' GeoNet strong motion stations (NZS1170.5:2004 site subsoil Class D; Standards New Zealand 2004; Table 1.1). Amplification factors in this period range reached greater than three with respect to rock at each of these recording sites (Bradley *et al.* 2018). Furthermore, the strongest amplification occurred in deeper parts of the basin, where spectral accelerations exceeded the 1 in 500-year return period design level (typical for ultimate limit state design). Amplification effects at similar periods were also observed during the 2013 Mw 6.6 Cook Strait and Lake Grassmere earthquakes, indicating that these effects are likely repeatable in future events (Holden *et al.* 2013; Bradley *et al.* 2018).

Detailed understanding of the 3D basin subsurface structure and key geotechnical properties is crucial to evaluate ground motions and damage patterns and inform robust engineering design practices going forward. Currently New Zealand structural design accommodates site and basin amplification effects largely through the New Zealand loadings standard (NZS 1170.5:2004; Standards New Zealand 2004) which categorises subsoil into discrete geotechnical classes A–E (Table 1.1, Table 1.2). In Wellington, the boundary between site subsoil Class C and Class D (equivalent to site period = 0.6s) runs through the central city (Semmens *et al.* 2010), creating a significant 'step' increase in design level and cost required for Class D sites. An alternative design option (McVerry 2011) based on low amplitude natural site period (Tsite) has also previously been proposed for Wellington in order to overcome this 'step' in design requirements. Hence, knowledge of this parameter is crucial to evaluate damage patterns and guide future mitigation efforts. Furthermore, a 3D basin velocity model is a critical first step to conducting ground motion simulations of past and future earthquake scenarios in order to understand and evaluate complex 2D and 3D basin effects and their future impact.

The first 3D basin model for central Wellington basin model (v1.0) was compiled by Semmens *et al.* (2010, 2011). Based on the 3D model and a small number of geophysical measurements, Semmens *et al.* (2010) also provided maps of key geotechnical parameters (e.g. surface geology, subsoil site class, site period, bedrock depth and Vs30[1]) and the distribution of underlying borehole and geophysical datasets. However, data coverage was sparse in some areas, particularly the deeper parts of the basin, with only a limited number of deep borehole measurements and geophysical data points available to guide development of the model. Since that research significant new data have been collected and are available for new iterations of that model.

In this work, we provide a new updated 3D geological and velocity model of the Wellington basin (v2.0). Our 3D basin model also includes updated surface geology and greywacke basement depth (equivalent to Z1.0[2] bedrock depth). Based on this model and new geophysical measurements we have also updated maps of the two key geotechnical parameters underpinning current Wellington design practice: NZS1170.5 subsoil site class and low amplitude natural site period (Tsite). The mapped area (shown in Figure 1.1C is expanded from that of Semmens *et al.* (2010) to include the Wellington Ferry Terminal to the north and beyond the Wellington Hospital to the south.

To underpin our new model and maps, we have compiled two significant new databases, that, include new data available since 2010:

- Updated borehole database including 700+ additional boreholes and numerous CPT/SPT and shear-wave velocity (Vs) measurements,
- New geophysical site period database including 400+ new measurements with associated uncertainty.

These databases have allowed us to better define the shallow subsurface layers (based largely on borehole and elevation data) and the deeper basin response (based largely on geophysical measurements). Although not intended to replace detailed site-specific assessment, this compilation provides an overview of spatial variations and key features within the Wellington basin on a block-by-block scale. Furthermore, details of the underlying data constraints and methodology are provided and discussed, to inform potential users of the robustness of the characterisation in different areas of the city.

In the following sections, we present an overview of the new data compilations, the 3D basin model (v2.0) and the development of updated site period and site class maps. We also highlight significant insights gained through this project since the work of Semmens *et al.* (2010) as well as areas of remaining uncertainty.

[1] Vs30 is the time-averaged shear-wave velocity in the top 30 m of the subsurface.
[2] Z1.0 is the depth to material with shear-wave velocity of 1km/s or greater.

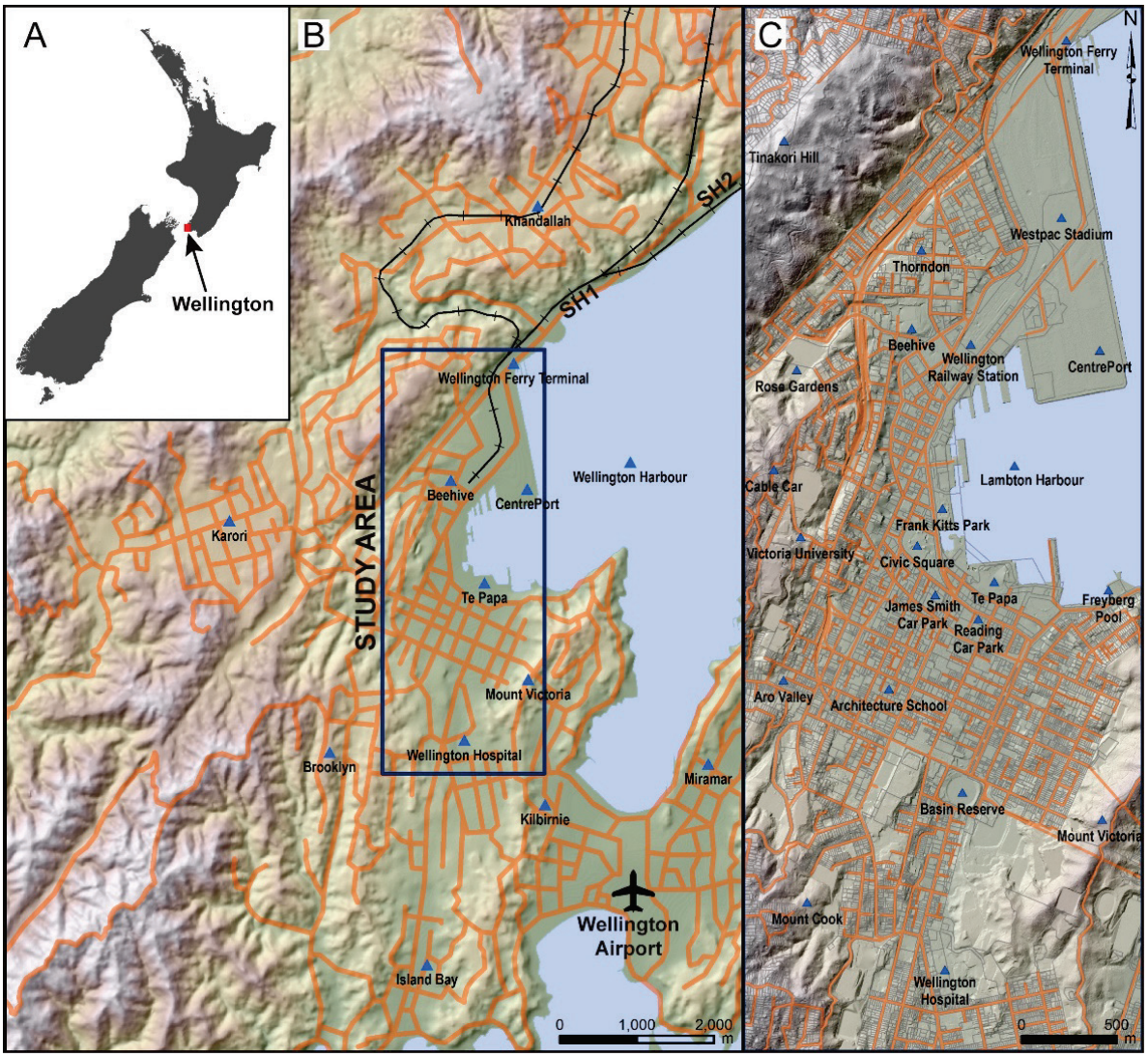

Figure 1.1 Location of study area in Wellington, New Zealand. A) Wellington's location within New Zealand; B) Wellington region showing study area, harbour, surround suburbs, regional road and rail network, and Wellington Airport; C) Study area (region of box in B) and key locations, roadways and built up areas.

Table 1.1 NZS 1170.5:2004 Site subsoil class definitions (Standards New Zealand 2004).

Site Subsoil Class	Description	Definition
A	Strong Rock	Unconfined compressive strength (UCS) > 50 MPa & Vs30 > 1500 m/s & Not underlain by < 18 MPa or Vs 600 m/s materials.
B	Rock	1 < UCS < 50 MPa & Vs30 > 360 m/s & Not underlain by < 0.8 MPa or Vs 300 m/s materials, A surface layer no more than 3 m depth of highly weathered (HW) or completely weathered (CW) rock or soil (a material with a UCS < 1 MPa).
C	Shallow Soil	Not class A, B or E, Low amplitude natural period ≤ 0.6s, or Have depths of soils not exceeding those in Table 2.
D	Deep or Soft Soil	Not class A, B or E, Low amplitude natural period > 0.6s, or Have depths of soils exceeding those in Table 2, or Underlain by < 10m soils with undrained shear strength < 12.5KPa, or < 10m soils SPT N < 6.
E	Very Soft Soil	> 10m soils with undrained shear strength < 12.5KPa, or > 10m soils with SPT N < 6, or > 10m soils with Vs ≤ 150m/s, or > 10m combined depth of above properties.

Table 1.2 NZS 1170.5:2004 Maximum depth limits for site subsoil class C (Standards New Zealand 2004).

Soil Type & Description		Max. Depth (m)
Cohesive Soil	Representative Undrained Shear Strength (KPa)	
Very Soft	< 12.5	0
Soft	12.5-25	20
Firm	25-50	25
Stiff	50-100	40
Very Stiff/Hard	100-200	60
Cohesionless Soil	Representative SPT N Values	
Very Loose	< 6	0
Loose Dry	6-10	40
Medium Dense	10-30	45
Dense	30-50	55
Very Dense	> 50	60
Gravels	> 30	100

2.0 KEY GEOTECHNICAL PARAMETERS

In this section, we define the key geotechnical parameters mapped in this study. Our approach to defining these parameters is consistent with the previous work of Semmens *et al.* (2010); the reader is referred to this work for additional details. Here we present a summary and note any deviations from the Semmens *et al.* (2010) approach.

2.1 Basin Engineering Geological Units and Shear-Wave Velocity

Our updated 3D Wellington geological and velocity model is based on the same geological classification scheme as Semmens *et al.* (2010) summarised in Table 2.1. This scheme groups "like" geological deposits into key engineering unit categories based around geological description and SPT N count values (which are a representation of the stiffness in non-cohesive materials). In addition to the Semmens classification, we have defined a new "Engineering Fill" unit, which was previously included within the "Soft/Loose Deposits" category. The separate characterisation of this unit was made possible by the additional density of shallow borehole data available since 2010. Furthermore, the delineation of engineering fill helps to define the extent of reclaimed land in waterfront areas and provides further insights into the effect of near-surface sediments on seismic response. A detailed definition of the mapped geological units and underpinning borehole database is included in Section 3.1.

We have adopted the shear-wave velocity characterisation of Semmens *et al.* (2010) for each unit in the 3D basin model (Table 2.1). A first review of new velocity information collected since 2010, suggest the average velocities assigned to each layer are appropriate to capture first order velocity variations. Hence, the 3D basin velocity model is constructed using the average Vs for each unit assigned uniformly to each geological layer. This is considered the most robust approach for the basin-scale model, given the inherent uncertainty and natural variation associated with such measurements (see minimum and maximum measured values). The new 'Engineering Fill' unit was assigned a velocity of 190 m/s, which is consistent with the approach in Semmens *et al.* (2010) of arbitrarily reducing the velocity of 'Soft/Loose Deposits' by 30 m/s within waterfront reclamation areas, based on known velocity profiles. Our velocity model has been validated by comparison of expected Tsite calculated from the 3D model with Tsite measured independently using geophysical methods (see Section 6.0).

Table 2.1 Summary of shear-wave velocity measurements by engineering geological unit for the Wellington CBD, modified from Semmens *et al.* (2010) to include the additional unit of Engineering Fill. The average shear-wave velocities were used in this study to estimate site period from the 3D basin model.

Engineering Geological Unit		No. of Tests	Test Types	Measured Shear-Wave Velocity (m/s)				
				Minimum	Maximum	Median	Average	Standard Deviation
Hydraulic Fill		13	SCPT	100	150	125	125	15
Engineering Fill Soft/Loose Deposits		112	SCPT, SPAC, ReMi & Down-Hole	105	385	205	190 220	55
Stiff/Dense Deposits	Total	61	SCPT, SPAC, ReMi & Down-Hole	220	570	390	400	80
	Upper (< 50 m depth)			320	480	n/a	400	n/a
	Lower (> 50 m depth)	n/a	Based on Fry et al. (2010)	470	730	n/a	600	n/a
Greywacke Bedrock		39	Seismic Refraction	365	1760	990	960	330

Test type definitions: SCPT = Seismic Cone Penetrometer Test, SPAC = SPatial Auto Correlation, ReMi = Refraction Microtremor & Down-Hole = Geophone Measurement in a Borehole.

2.2 Site Period (Tsite)

The low amplitude natural site period (Tsite) is the fundamental period of vibration of the soil column above rock at that site. This period can be estimated using approaches that reconstruct the 1D shear-wave velocity profile below the site down to bedrock, or alternatively measured directly from ambient vibrations recorded at the surface. We use three primary approaches to characterise Tsite, listed below in order of preference as defined by proposed guidance (NZS 1170.5 A1:2016, Standards New Zealand 2016):

i. Direct measurements of shear-wave travel times/velocities from downhole geophysical investigations. These are available at a small number of sites in our study.

ii. Shear-wave velocities and geological profiles determined through a combination of geological log constraints and geophysical measurements at the site or nearby sites. In practice, this allows us to calculate Tsite values from the 3D geological layer model with assigned shear-wave velocities as detailed in Section 2.1.

iii. horizontal-to-vertical spectral ratio technique (HVSR; e.g. Nakamura 1989). These geophysical measurements use recorded microtremor vibrations and do not rely on detailed knowledge of the subsurface structure.

Details of the measurement techniques and underlying data are included in Section 3.2. In practice, to estimate Tsite from 1D shear-wave velocity profiles (i. and ii. above), we use the commonly used four-way travel-time (4WTT) simplification, where the travel-time contributions of each geological layer are summed, using estimates of thickness and Vs for each layer down to bedrock. Based on average shear-wave velocities in Table 2.1, bedrock depth for Wellington can be assumed to be equivalent to the depth to greywacke basement. It is possible that in the deeper parts of the Thorndon basin (e.g. CentrePort area) greywacke basement is overlain by older sedimentary deposits that could be classed as engineering bedrock; however, the lack of deep borehole information in this area means that this cannot yet be clarified or incorporated into our model.

We note, that the period of peak amplification measured directly from ground motion data (iii. above) may differ in some cases from the 1D profile estimate due to simplifications associated with the 1D profile, or the presence of 3D amplification effects arising from more complex surrounding subsurface structure; on the other hand geophysical measurements of site period based on spectral ratios (e.g. HVSR) may also be affected by the presence of amplification on the denominator (e.g. vertical amplification in the case of HVSR).

However, in Wellington we generally see reasonably good agreement across the approaches (i) to (iii) above. For some sites with steeply dipping basement topography at the basin edge, the site period measured from HVSR (iii above) is somewhat longer than that measured by techniques (i) and (ii); we infer this is due to 2D/3D basin amplification effects. In these cases, we have adopted the results of (i) and (ii) only where shallow boreholes down to greywacke basement are present nearby; with technique (iii) adopted where basement depth is not well constrained. More details are presented in Section 6.0.

2.3 Site Subsoil Classification (NZS1170.5: 2004)

New Zealand's NZS1170.5 loadings standard prescribes five discrete subsoil categories A–E, which are defined according to the criteria in Table 1.1 and Table 1.2. In the Wellington region, greywacke basement outcropping in the hills surrounding the basin, is designated as Class B (soft rock; e.g. Semmens *et al.* 2010). Soils within the Wellington basin range from Class C (shallow soil) – Class E (very soft soil).

In this study, we take a practical approach to block-by-block site class mapping based on the available geological and geotechnical datasets, detailed in Section 6.1. This can be summarised as follows:

- Class B/C boundary is defined using the 3 m depth-to-greywacke contour extracted from the 3D basin model.
- Class C/D boundary is based on Tsite = 0.6 s and is consistent with the approach of Semmens *et al.* (2010).
- A possible area of Class E is flagged where hydraulic fill is present and/or historical liquefaction has been observed. We note the original intent of the Class E standard was to capture liquefiable sites, and these are clearly present within this area. Recent Vs measurements here also support Class E classification and further investigations are underway.

Our new site class maps do not replace detailed site-specific investigation for individual building design. We note, that such detailed site-specific studies can yield additional geotechnical parameters which allow more complete assessment of suitable design practice.

2.4 Z1.0

Site-specific seismic hazard studies using modern best-practice ground motion prediction equations (GMPE) require an estimate of Z1.0 (depth at which material ≥ 1.0 km/s is encountered). In Wellington, available Vs data (summarised in Table 2.1 and Semmens *et al.* 2010) suggest that the depth to greywacke basement is a good proxy for the Z1.0 parameter. We note, that the shear-wave velocity of greywacke may be reduced below 1.0 km/s if moderate to highly weathered (Semmens *et al.* 2010), such that if a thick weathering layer exists below a site, Z1.0 may be somewhat deeper than this value in practice. The shear-wave velocity of stiff/dense deposits in the Wellington basin modelled in this project is less than 1km/s.

In this study we provide updated maps of Bedrock Depth (depth to greywacke basement) extracted from the 3D basin model that can be used as a first order estimate of Z1.0 depth.

2.5 Vs30

Site-specific hazard studies also require an estimate of Vs30. In this study, we do not specifically update the Semmens *et al.* (2010) Vs30 map, given the current density of shallow Vs30 measurements is not sufficient to robustly map subtle lateral Vs30 variations on a block-by-block scale. However, estimates of Vs30 can be extracted from the 3D model as an initial guide.

3.0 NEW DATABASES

Two new databases have been compiled under this project and are described in this section. These comprise an expanded borehole database for central Wellington and a new geophysical site period database based largely on HVSR measurements.

3.1 Borehole Database

3.1.1 Database Development

Borehole data for this project was primarily compiled from data within Semmens (2010), GNS Science drill hole records, the New Zealand Geotechnical Database (NZGD; https://www.nzgd.org.nz). A database was developed for the Wellington central borehole records so that all data captured for the project could be contained in a single location, be easily updated, and accessed by several software suites. The database was designed around a relational table system common to borehole or drill hole databases used in New Zealand and Australia; in particular, the design was based around a format suitable for easy importing of data into modern 3D geological modelling software. The database was also designed around version four of the electronic transfer standards published by the Association of Geotechnical and Geo-Environment Specialists (AGS4) and the New Zealand Geotechnical Society (NZGS) (Anderson *et al.* 2017).

Data from Semmens (2010) was upgraded into the new database format and some additional interpretations and classifications of lithology were also completed for these records. Some drill hole records held by GNS Science were added to the database; from these, geological, geotechnical and geophysical information from digital scans of paper records were digitised and compiled. Several hundred new borehole records were also digitised from PDF logs held by the NZGD, a geotechnical borehole and data repository administered by MBIE; MBIE commissioned work to expand the NZGD database and make privately held data available following the Kaikōura earthquake. Additional borehole data may be privately held by geotechnical companies that have worked in the Wellington region and not yet available through the NZGD; a small number of such records were included where known, but such records were not directly sought through this project.

The database is comprised of six tables; a borehole location or collar table, a down-hole lithology description table; a down-hole standard penetrometer test (SPT) measurement table; a down-hole shear-wave velocity measurement table; a down-hole cone penetrometer test (CPT) measurement table; and a hole orientation or survey table. All down-hole tables are linked back to the borehole location table with a unique borehole ID number within the LOCA_INDEX field. A summary of the data captured for this project is provided in Table 3.1. The data from these borehole records were used to develop 3D geological models of the subsurface.

Table 3.1 Summary of data types in the borehole database.

Table	Description	Semmens (2010)	GNS Science	NZGD
LOCA	The location or collar table that contains borehole coordinates, depth, water, and details about the owner and drilling company.	n=983	n=70	n=541
HORN	The hole orientation or survey table.	n=983	n=70	n=541
GEOL	Down-hole lithology descriptions and interpretations for borehole intervals.	n=7,515	n=1,479	n=8,818
SPT	Down-hole SPT measurements.	n=4,892	n=324	n=3,848
CPT	Down-hole CPT measurements.	Nil	Nil	n=28,816
VELOCITY	Down-hole shear wave velocity measurements or calculations.	Nil	n=181	n=136

Lithological descriptions, weathering, and SPT, CPT or shear wave velocity analyses were extracted from borehole records and entered into the database verbatim from the original logs. An interpretation of the primary and secondary lithological type from using NZGS standards was made for each lithological description; and in most cases, an interpretation of the geological formation and group was also made. To assist with mapping and further interpretation of the data, occurrences of shells, peat or wood were noted in the project specific data fields. In addition, each down-hole interval within the lithology table was classified into one of nineteen lithotechnical subgroups defined by Semmens *et al.* (2010) and summarised in Table 3.2. Data-mining was completed in clusters of 50–100 boreholes and upon completion the data was visually quality checked for entry errors and digitally quality checked within Leapfrog Geo 3D modelling software for drill hole ambiguities (e.g. interval overlaps, repeated boreholes, or shortfalls in final depth). Once the quality checking was completed data was appended into the master Microsoft Access™ Database.

Table 3.2 Engineering classes after Semmens *et al.* (2010).

Name	Lithotechnical Unit Code	Group
Hydraulic Fill	FP	Fill
Soft Deposits - end dumped fill	FE	
Soft Deposits - swamp deposits	LS	Loose Deposits
Soft Deposits - undifferentiated silts and clays	LF	
Loose Deposits - beach or shallow marine	LB	
Loose Deposits - alluvial deposits	LA	
Loose Deposits - colluvial deposits	LC	
Loose Deposits - undifferentiated sediments	LU	
Stiff Deposits - clays	SL	Stiff Deposits
Stiff Deposits - silts	SS	
Dense Deposits - fine interbedded sediments	SI	
Dense Deposits - alluvial deposits	SA	
Dense Deposits - colluvial deposits	SC	
Dense Deposits - undifferentiated sediments	SU	
Greywacke basement - weathered	RW	Greywacke
Greywacke basement — unweathered	RR	
Greywacke basement — unknown weathering grade	RU	
Water	H2O	Other
Unknown / no core	UK	

For this study a total of 17,182 lithological descriptions from 1,594 boreholes were available in the database along with 9,064 SPT, 28,816 CPT and 317 shear wave velocity measurements. These boreholes are predominantly located within the Wellington CBD (Figure 3.1a) and areas of development over the last century. The longest borehole in the study area is located at Te Papa and was 152.3 m. Other deeper boreholes are located along the harbour edge in thicker sediment and shallower holes closer to the Wellington Basin margin (Figure 3.1b). Most of the boreholes are less than 20 m in depth (Figure 3.2a) and most boreholes were drilled between 1937 and 2017 (Figure 3.2b).

3.1.2 Borehole Quality

For this project each borehole in the database was assessed for quality. The original borehole logs were analysed and given a subjective ranking between one and five with five being of a very high quality. This guided subjective rank score is summarised in Table 3.3. Most of the boreholes in this study were high quality geotechnical engineering logs with rank scores of four and five (Figure 3.2c). This rank score can be used in the geological modelling to assess the confidence of borehole data and is used in this study to assess the uncertainty in the 3D geological modelling.

Table 3.3 Ranking scheme for the borehole quality.

Score	Description	Example NZGD Borehole
1	Basic grain size and lithology information recorded, but with abundant generalisation.	Other_78907 Other_78531
2	Lithology, colour and grain size recorded with more geological variability described, but not well separated into specific intervals.	Other_81161 Other_79405
3	Lithology, grain size and colour with some hardness information recorded for most sections. Includes some local geological unit or formation names. Some terminology and names may be misinterpreted or do not correlate with adjacent holes.	Other_81681 Other_90026
4	Detailed descriptions, geological units identified, and unit boundaries are clear. Some information may be unclear due to poor logging quality or scanning.	Other_78651 Other_82551
5	Advanced terminology, very good detailed descriptions, geological units and boundaries identified, and logs plotted using professional data visualisation software.	BH_65899 BH_89599
-99	Rank score not applied due to missing information.	E.g. Boreholes from Semmens (2010) without original logs available for QA.

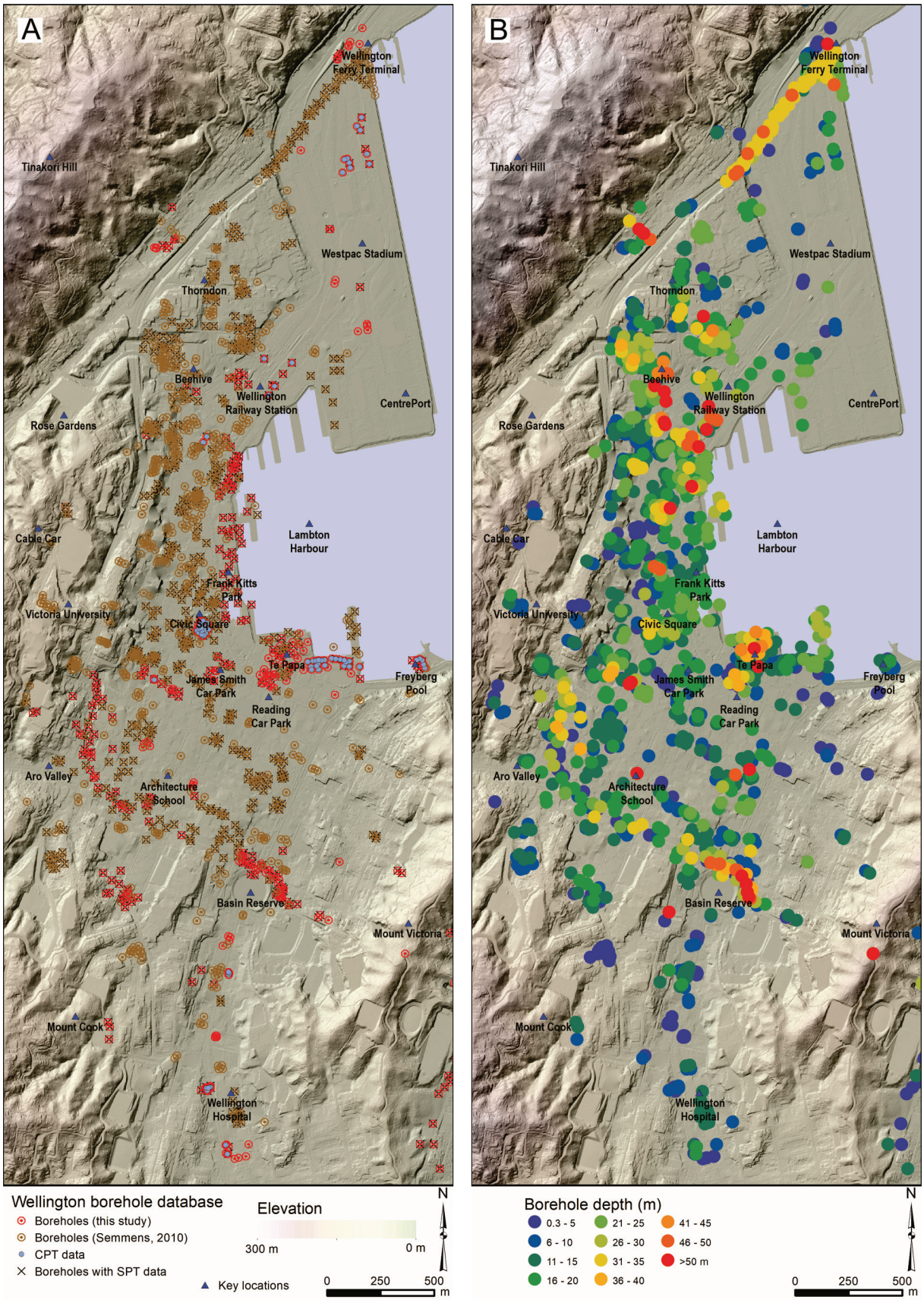

Figure 3.1 Location of boreholes with geological and geotechnical data used in this study. A) locations of new borehole data captured for this study, previous borehole data (Semmens, 2010), SPT data and CPT data; B) depth of boreholes in the study area (check JSCP Aurecon hole).

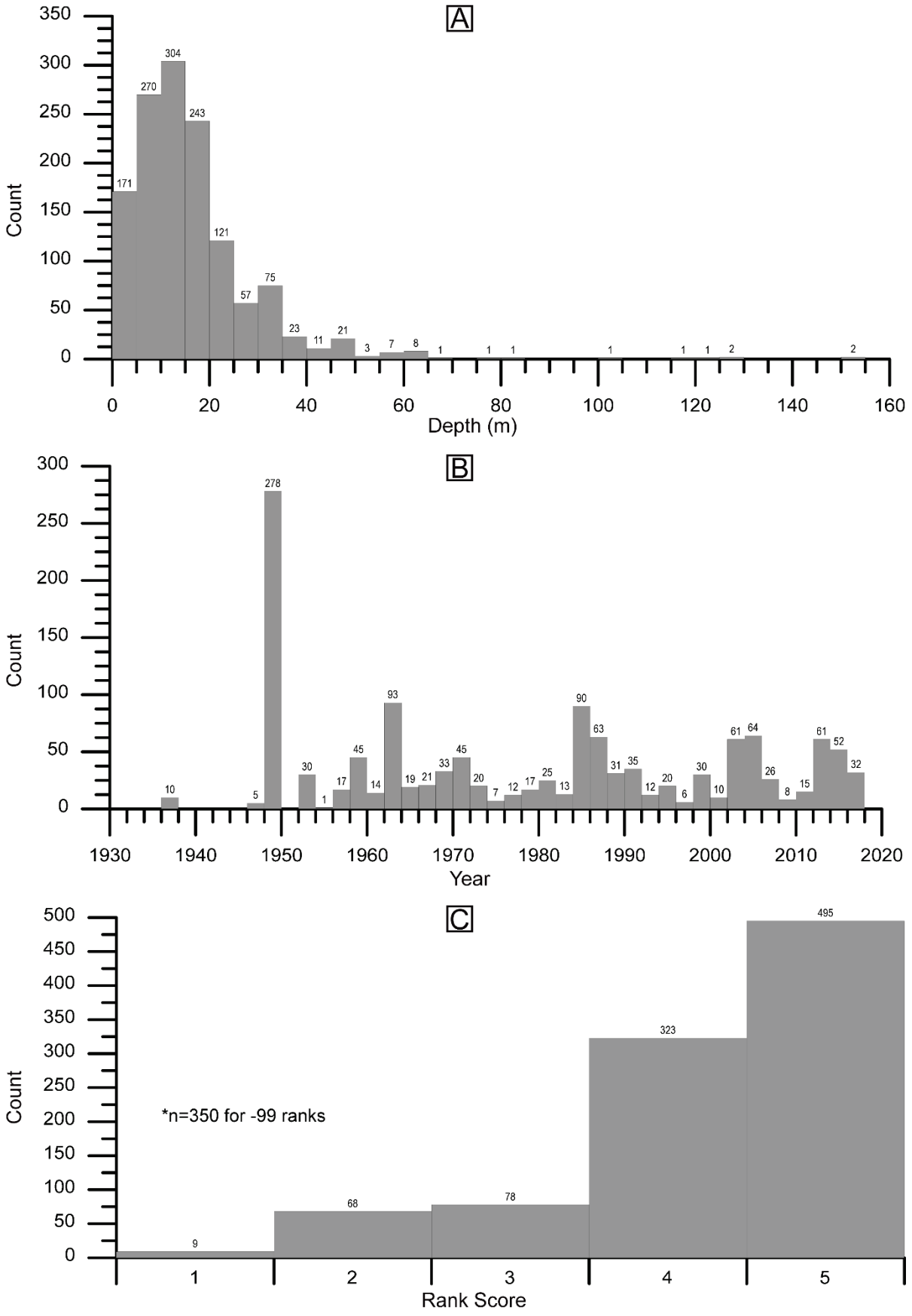

Figure 3.2 Histogram plots of borehole data statistics. A) Range of borehole depths in the Wellington central study area; B) Year that borehole was drilled; C) Rank Score that represents borehole log quality.

3.1.3 Database Overview

Analyses from the borehole database can be made in GIS software that aid our interpretation of the subsurface geology as well as identification of potential gaps in the borehole data coverage. Plots of depth to the basement and where boreholes are drilled to that depth (Figure 3.3a); or the thickness of the man-made fill, are all particularly useful for this study (Figure 3.3b). Only 429 of the 1,427 boreholes in the database intersected the basement. There are many parts of the study area that we therefore have poor constraints on the depth to basement such at the Thorndon area, Wellington Stadium / CentrePort, and from Wellington Railway Station south to Frank Kitts Park. The engineered or hydraulic fill in the study area is concentrated near the Wellington CBD can be seen at its thickest near the harbour shoreline and thinning inland. Semmens *et al.* (2010) provide a good summary of the fill deposition timing and locations.

The new borehole database underpins the development of the 3D geological model, described in Section 5.0.

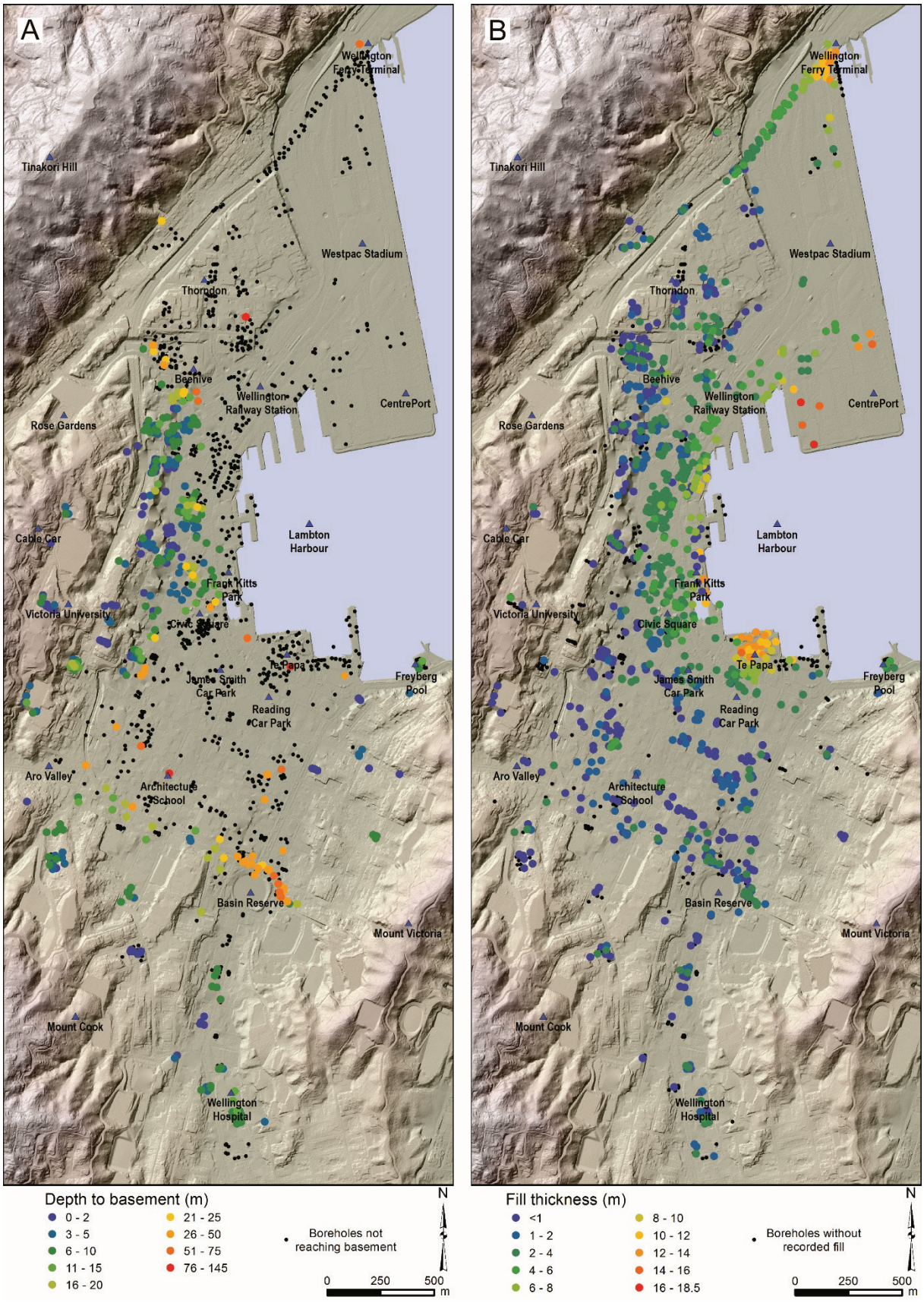

Figure 3.3 Boreholes that reached basement (A) and thickness of hydraulic or engineered fill in boreholes (B).

3.2 Geophysical Site Period Database

GNS Science, the University of Auckland and collaborators from the University of Texas at Austin have collated over 483 geophysical site period measurements in the central city (Figures 3.4 & 3.5). The majority of these measurements have been derived from analysis of seismometer recordings of ambient noise at closely spaced locations using the horizontal-to-vertical spectral ratio (HVSR) technique (Nakamura 1989). Our geophysical surveys have largely targeted the deeper parts of the Wellington basin (i.e.> 30 m of sediment), where borehole information down to greywacke basement is sparse. In these locations, clear amplification peaks in the HVSR data are observed in many cases, and these can be used to estimate the site period. Hence the site period database is directly complementary to the borehole database described in Section 3.1.

The database has been compiled as far as practical with common processing techniques and evaluation criteria. A minority of measurements from older site surveys (collected prior to this study) have used alternative processing schemes, and have been noted accordingly

3.2.1 New HVSR Measurements

Portable seismometers were installed temporarily in Wellington by the University of Auckland/University of Texas and GNS Science at ~390 new HVSR sites to ensure block-by-block coverage of the central city basin. These instruments recorded ambient noise for periods of approximately 30 mins to 3 hours and were installed within the period December 2016–October 2017. The recording instruments were a combination of Trillium compact broadband instruments and 1s Lennartz instruments connected to Taurus/Centaur digitisers. These were supplemented by University of Auckland 2 Hz 3 component geophones (Mark Products) connected to dynamic signal analysers (Data Physics Quattro).

HVSR analysis was conducted using geopsy software (www.geopsy.org) with some refinement of University of Auckland data using Matlab software. Data showing excessive incoherent noise from near-field signals (through-going traffic, occupation/building plant signals) and earthquakes were excluded from the analysis. Single HVSR curves were calculated from multiple 50 - 200 s data windows applied to each ambient noise record. The squared average (quadratic mean) of the horizontal components and geopsy default smoothing of type Konno & Ohmachi (1998) with constant of 40 were used to derive the single HVSR curves for each window. The single HVSR curves were then smoothed and averaged to yield a mean HVSR curve and its standard deviation. For each site, the number of samples in the selected data ensures a sufficient number of cycles at the periods of interest are represented in the mean HVSR curve (e.g. SESAME guidelines; Accerra et al. 2004).

For each site, a mean resonance frequency f_0 (inverse of the fundamental site period) and its standard deviation were derived using automated algorithms from the ensemble of single HVSR curves. The amplitude of the peak was estimated from the mean HVSR curve at the peak frequency f_0. In cases where more than one HVSR peak was identified, the frequency and amplitude of each peak were automatically estimated. A preferred amplification peak was then chosen, based on qualitative user interpretation that also considered all available data near that location to determine the most likely site period down to greywacke basement. As expected for the natural (fundamental) site period, in most cases the preferred peak was the lower period peak. However, there were a small number of cases when a low-amplitude peak at long periods was present, but was not compatible with known basement depth in boreholes; in these cases this peak was assumed to arise from other factors, e.g. 3D basin or topographic response or noise contamination, and was discarded from the Tsite analysis.

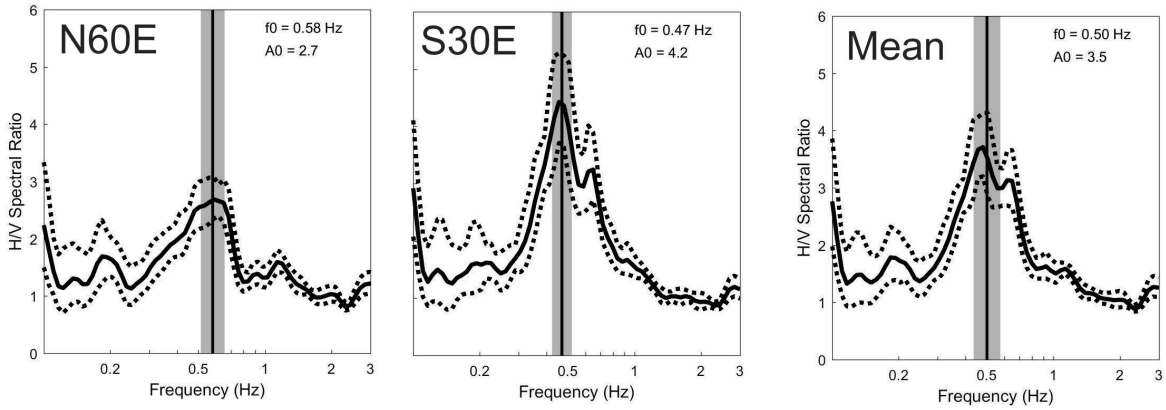

Figure 3.4 Example HVSR curve calculated for individual horizontal components (azimuths N60E, S30E), as well as the mean horizontal component adopted for this study.

In many cases, significant polarization of an amplification peak was observed, which is indicative of complex 2D/3D effects. Polarisation is shown by variation in the peak period and/or amplitude of the HVSR curve depending on the horizontal azimuth of the recording component at that station (e.g. Figure 3.4). In our database, we capture the dominant azimuth of polarization for each observed HVSR peak where practical. This was estimated by identifying the azimuth of the maximum amplitude within one standard deviation of f_0 from a suite of HVSR curves calculated for horizontal azimuths spaced every 10 degrees. Furthermore, we consider azimuthal variations of amplification to aid interpretation of the data at sites where considerable spatial complexity in site period was observed. However, for practical reasons, we use the squared average horizontal component HVSR curves to determine the representative site period recorded in the database.

Table 3.4 Key parameters included in the geophysical site period database for each site period measurement (where available).

Parameter		Description
Station Name		Unique recording site identifier
Measurement type		HVSR in most cases, but also includes some measurements derived from downhole Vs surveys, ReMi Vs profiles etc.
Instrument details		Instrument type and recording times (if applicable)
Agency		Source of data (e.g. GNS Science, University of Auckland etc.)
For each identified amplification peak	Fpeak ± one standard deviation	Frequency of the amplification peak and its standard deviation
	Apeak ± one standard deviation	Amplitude of the amplification peak and its standard deviation (where available)
	Dominant azimuth	Dominant azimuth of the amplification peak (where available)
	Clarity criteria check	TRUE or FALSE depending on whether the peak satisfies clarity criteria given in the European SESAME H/V user guidelines (Acerra *et al.* 2004).
	Reliability criteria matched	Number of reliability criteria satisfied (out of a total of 6) as defined by the European SESAME H/V user guidelines (Acerra *et al.* 2004).
Tsite		Period of preferred amplification peak
Weight		Measure of Tsite robustness ranging from 0 (unusable) to 5 (best) as described in Section 3.2.2.

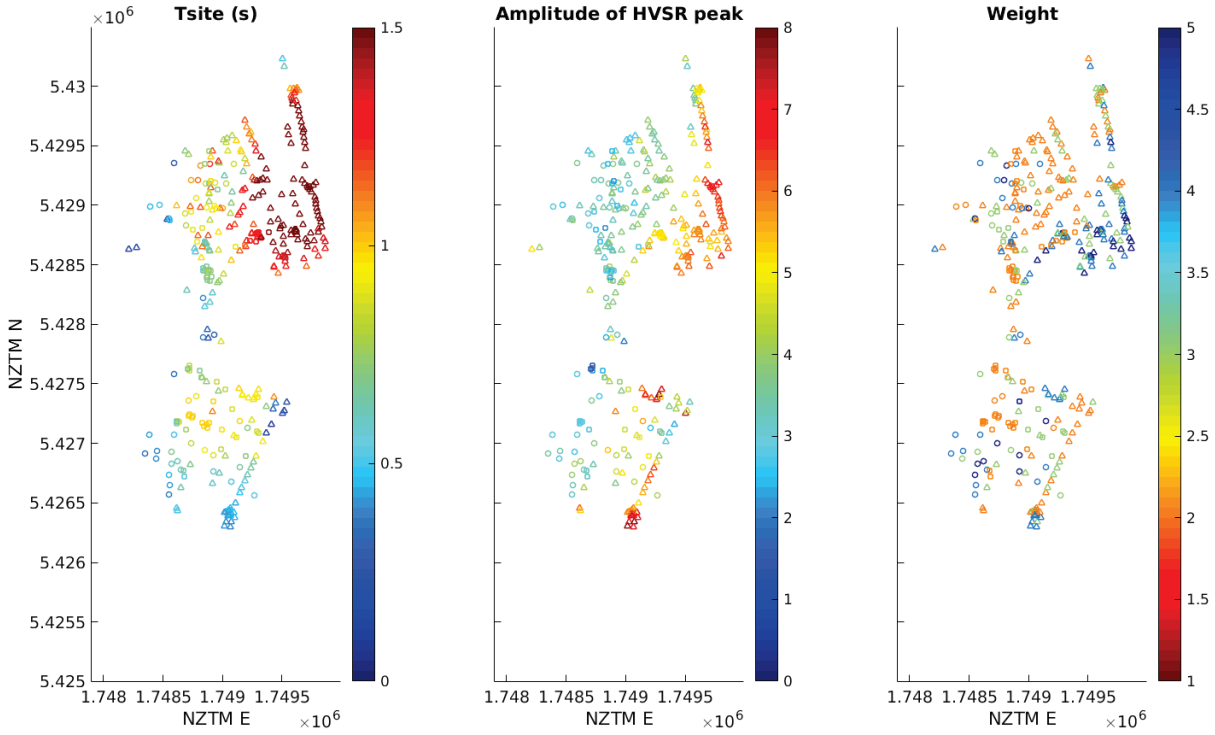

Figure 3.5 Summary of Tsite values from the site period database and corresponding amplification (amplitude) values. The symbol shape indicates the source of the measurement as follows: square=existing GNS; circle=new GNS; triangle=new UOA. Note, that existing GNS Tsite amplitude measurements have been scaled to be compatible with the quadratic mean as described in the text.

3.2.2 Site Period Uncertainty

For each measurement in the site period database, an additional summary measure of overall uncertainty or 'Weight' (W) is also given where categories are as follows: 0=unusable, 1=very poor, 2=poor, 3=satisfactory, 4=good, 5=excellent. These values enable the relative robustness of each measurement to be captured in a consistent manner and supplement the standard deviation values given separately for each amplification peak. The 'Weight' values also facilitate interpretation of closely spaced measurements which may differ,

The 'Weight' value is calculated by combining both quantitative and qualitative assessment of measurement robustness. Firstly, the quantitative score (QN) ranges from 0 to 6 equivalent to the 'Reliability criteria matched' (Table 3.4) for the preferred amplification peak. Secondly, a qualitative confidence measure (QL) ranging from 0 to 1 is assigned to each measurement using the following guide outlined in Table 3.5.

These scores are then combined using a simple formula to produce a final Weight (W) rounded to the nearest integer value:

$$W = (QN - 1) * QL$$

Table 3.5 Examples of qualitative quality assessment scheme for site period measurements.

Qualitative confidence (QL)	
0	HVSR peak amplitude < 2.5 and/or No peak lies within range of credible fundamental period values associated with local soil deposits (e.g. Peaks observed at rock sites that are likely topographic in origin) Faulty sensor or recording
0.25	Multiple peaks are present, and interpretation is ambiguous
0.5	More than one amplification peak present and preferred peak can be identified, but is uncertain
0.75	Clearly preferred amplification peak consistent with known subsurface structure, but with uncertainty in period due to noise or broad/complex amplification response
1	Clearly preferred and well-defined amplification peak that is consistent with expected subsurface structure

3.2.3 Other Data Sources

Additional site period estimates collated in the database include:

i. Previous site studies conducted by GNS Science, many of which used the alternative HVSR processing scheme of Beetham *et al.* (2010). For these measurements, a 'Weight' was not quantitatively extracted, but was assigned using W = QL * 5 rounded to the nearest integer, resulting in assigned values ranging from 0 to 5. For these sites, the processing scheme used vector summation of the two horizontal components to derive amplitude; hence for these sites the amplification value has been scaled downwards by √2, to be compatible with the quadratic mean approach (e.g. Albarello & Lunedei 2013).

ii. Previous ReMi studies (A. Kaiser & J. Louie 2006 unpublished data) also included in the Semmens *et al.* (2010) compilation. Site period has been estimated using the 1D Vs profile derived at the site and qualitatively assigned a 'Weight' of 1 or 2.

iii. Two estimates based on the downhole Vs measurements by adopting a representative simplified 1D layered velocity profile. These have been individually assessed and assigned a qualitative 'Weight' of 4 or 5.

iv. Unpublished HVSR and SSR analysis of earthquake ground motion at GeoNet strong motion stations (e.g. those used in Kaiser *et al.* 2017b). These values have been individually assessed and assigned a qualitative 'Weight' of 2 or 3.

3.2.4 Database Overview

An overview of the database values is given in Figure 3.5 and Figure 3.6. The values of Tsite and amplitude are generally consistent across the different measurement types; we note that no significant bias due to different processing techniques is apparent Figure 3.5).

New measurements collected in the deeper parts of the Thorndon and Te Aro basins generally show clear amplification peaks leading to high 'Weight' values; these provide good constraints on the site period in areas where deep boreholes are sparse. We find that in the Te Aro basin to the south, the data illustrate a relatively simple pattern of site period variation within a steep-sided basin structure. However, variable and complex site amplification effects are observed within the Thorndon Basin to the north, which is bounded by the Wellington Fault. Our results suggest that the depth to greywacke basement may be deeper here than originally mapped in Semmens *et al.* (2010) and/or the presence of complex 3D basin-edge amplification effects may be complicating ground shaking patterns.

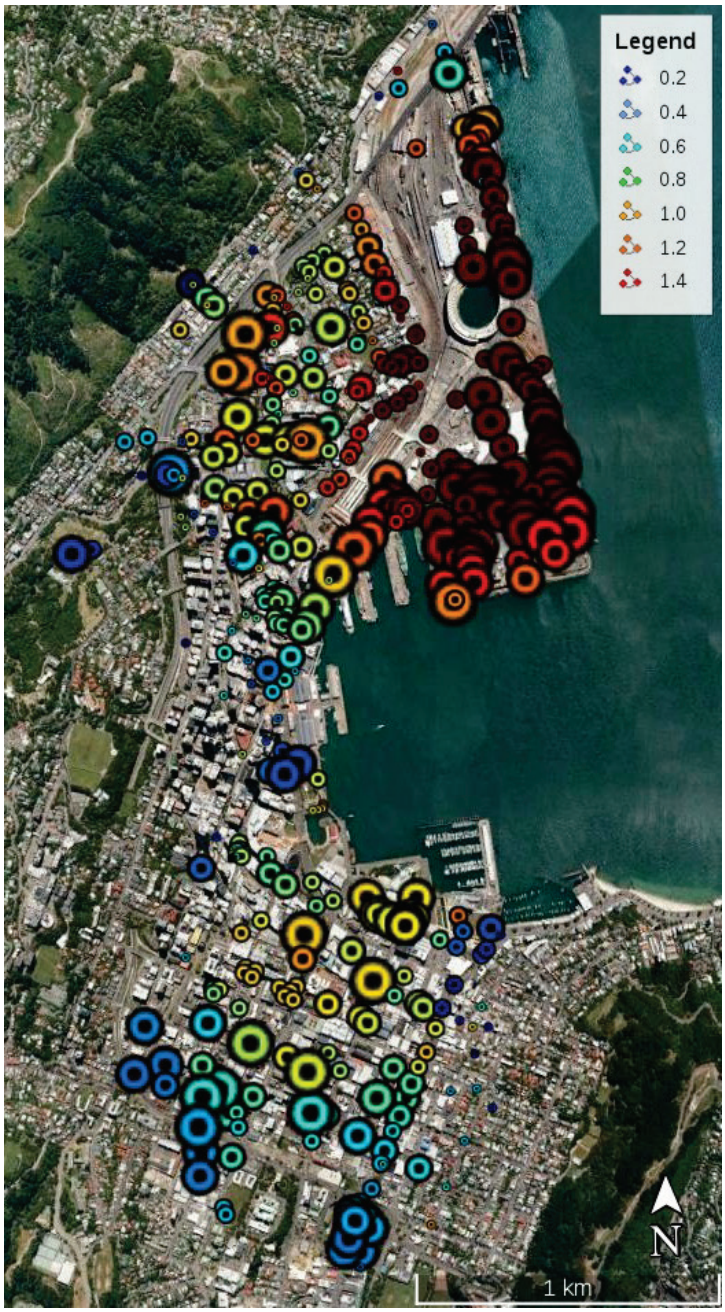

Figure 3.6 Location of measurements in the site period database. Colour indicates the site period value in seconds (see legend) and size indicates the relative robustness of the measurement (W).

4.0 GEOLOGICAL MAP

The geological map was updated from that compiled by Semmens *et al.* (2010; Figure 4.1a), that was based on the mapping by Begg and Mazengarb (1996) and Begg and Johnston (2000). Lithological units were based on those by Semmens *et al.* (2010) which reflect the variations in both depositional environment, timing of deposition and importantly the engineering properties of the deposits. Interpretations for the map in this project were extended to fill the new expanded study area in this project (outlined in Figure 1.1).

Integrated and interpreted desktop mapping was completed for this project (Figure 1.1b). The extended and updated interpretations were derived from new borehole data describing the near-surface sediments, high-resolution aerial photography (Figure 4.2) and high-resolution LiDAR digital terrain models (DTM) (LINZ 2013); all of which were not available at the time of previous mapping. Aerial photographs from the 1938 and 1954 (e.g. Figure 4.2a) were also available for the study area and provided information on areas of cut and fill that were integrated into this new map. Fault data was compiled from Begg and Mazengarb (1996) with the best mapped location of the Wellington Fault compiled from the Active Faults Database (Langridge *et al.*, 2016). The location and importance of the new Aotea Fault as an active seismic structure (Barnes *et al.*, 2014; Barnes *et al.* 2018) was a new addition to this map compared to previous interpretations. The trace of the Aotea Fault was continued onshore from marine seismic mapping using basement contacts in the borehole database, existing interpretations from Begg and Mazengarb (1996), and HVSR geophysical measurements. The location of the Aotea Fault onshore between Te Aro and Mount Victoria is less well constrained and based on Begg and Mazengarb (1996). Figure 4.1b and the geological modelling in this study only includes the two active faults in the region (the Aotea and Wellington faults), other faults in the study area such as those shown in Figure 4.1a and in Begg and Mazengarb (1996) are inactive and displacement on them cannot be resolved from data in this study. Data available on the generations and regions of manmade fill adjacent to the Wellington Harbour were also integrated from Semmens *et al.* (2010). All mapping data was compiled in ArcGIS and the final interpretation is provided in Figure 4.1b.

A summary of the stratigraphy used in this project is provided in Table 4.1. The geological units are those of Semmens *et al.* (2010) and are correlated as best possible to those of Begg and Mazengarb (1996) and the current New Zealand Stratigraphic Lexicon (Mortimer et al, 2016; Strong *et al.*, 2016). The study area consists of a sequence of Pleistocene to Holocene sediments deposited on the basement Rakaia Terrane sedimentary deposits from the Torlesse Supergroup. Holocene sediments include manmade fill; alluvial sand, silt and gravels; marginal marine mud and silts (commonly including macro fossils); colluvium consisting of gravels, sands and muds; and peaty swamp deposits. The older Pleistocene sediments include alluvial, colluvium and marine sediments. The Wellington Basin has accumulated a substantial thickness of Quaternary sediments with estimates of up to 600 m in the last 450 ka (Wood and Davy, 1992). Sedimentation is controlled not only by fault bounded depressions but also by localised folding east of the Wellington Fault (Begg and Mazengarb, 1996).

Table 4.1 Summary of stratigraphy used in this study compared with other publications.

This study	NZ Stratigraphic Lexicon	Begg and Mazengarb	Semmens *et al.*
Holocene - Hydraulic fill	OIS1 (Holocene) reclaimed land (Q1.antrec)	Reclamation landfill (fr)	Hydraulic reclamation fill, pumped sea bed sediments (sand, mud, gravel, shells (frh)
Holocene - Engineered fill	OIS1 (Holocene) engineered fill (Q1.anteng)		Reclamation landfill, gravel, sand, clay, silt, building debris (fr)
Holocene - Alluvium	OIS1 (Holocene) river deposits (Q1.alvgvl)	Alluvium (fa)	Alluvium (fa)
Holocene - Colluvium	OIS1 (Holocene) landslide deposits (Q1.lndbrc) or OIS1 (Holocene) fan deposits (Q1.fangvl)	Fan deposits (ff)	Colluvium, gravel, loess, tephra, peat, (fa+lg)
Holocene - Swamp	OIS1 (Holocene) swamp deposits (Q1.swp)	Swamp / peat deposits (fs)	Alluvium, silt, peat (ls)
Holocene - Marginal marine	OIS1 (Holocene) ocean beach deposits (Q1.bch)	Marginal marine sediments (fm)	Marginal marine deposits including esturine and beach sediments containing sand, shells, gravel, silts and clays (fm)
Pleistocene - Alluvium	Undifferentiated Pleistocene - Holocene river deposits (Q.alvgvl) or OIS11 (Middle Pleistocene) ocean beach deposits (Q11.bch)	Alluvium (ln)	Alluvium including subsurface gravels, solifluxion deposits, loess, swamp sediments, minor tephra (ln)
Mesozoic - Greywacke basement	Undifferentiated Rakaia Terrane Triassic sandstone and mudstone (Tr.szm)	Torlesse Complex (tw)	Alternating sandstone and argillite (tw)

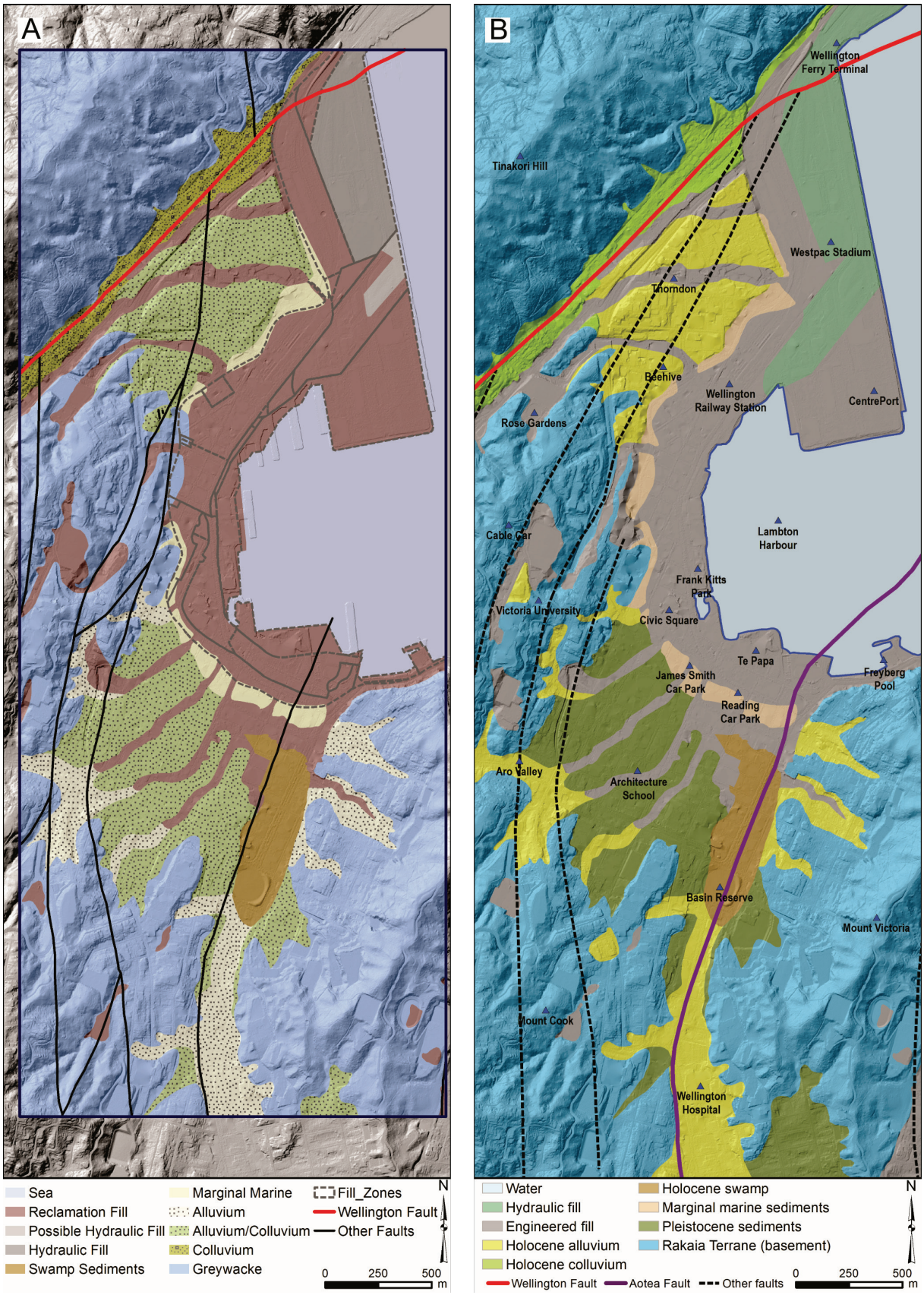

Figure 4.1 New geological mapping. A) geological map compiled by Semmens (2010); B) updated geological map compiled for this study, based on the Semmens (2010) and the Begg & Mazengarb (1996) maps with boundaries updated from aerial photography, LiDAR DTM models and the Active Faults Database (Langridge *et al.* 2016).

Figure 4.2 Historic aerial photographs of the study area. A) Historic aerial photography from 1938 (Survey 70); B) high-resolution urban aerial photography from 2016–2017.

5.0 3D GEOLOGICAL MODEL

The 3D geological model for this study builds on previous modelling by Semmens *et al.* (2010). The aim of this project was to provide a new iteration of the previous model using new borehole data, improved surface mapping from LiDAR elevation data and borehole records, and geophysical observations. The addition of the Aotea Fault as an active and basin bounding structure was a significant addition to the 3D geological model. New versions of the modelling software have also improved the geological model allowing for more integration of different datasets and faster interpolation at better cell resolutions. The resulting model can be used to analyse sedimentary unit thicknesses, calculate depth to basement, and can be used to create a 3D velocity model. Confidence factors for key data sets have been combined in 3D to provide an uncertainty model.

5.1 Model Development

The 3D geological modelled for this study was created with Leapfrog Geo 4.4. Surface elevation, geological mapping, geophysical and borehole data was imported into the model workspace from GIS and Microsoft Access™ databases. Other data that was used to constrain some contacts was digitised directly into the Leapfrog Geo workspace. Modelling of the top surface for each of the geological units was performed from the datasets and combined into a geological model using deposit or erosional relationships. The model was divided into three blocks by the Aotea and Wellington faults. The Mount Victoria block (east of the Aotea Fault), the CBD block (between the Aotea and Wellington faults) and the Tinakori Hill block (west of the Wellington Fault). Modelling was carried out within each block, and for most of the geological units in the model, only data that fell within a block was used in the computations of the surfaces. The model was created with a minimum 1,747,900 and maximum 1,750,000 easting; a minimum 5,425,000 and maximum 5,430,500 northing; and a -250 m minimum and 350 m maximum elevation (Z). The model was compiled at a 40 m triangulation resolution.

Seven geological units were used in this geological modelling (Table 5.1). These represent the engineering geological units of Semmens *et al.* (2010) and are derived from the same lithotechnical codes of that work. The exception in our model however is the inclusion of a new differentiation between hydraulic and engineered fill.

Table 5.1 Geological units used in the 3D model.

Unit	Code	Description
Water	WT	Wellington Harbour, mapped to include areas of floating or elevated wharfs. Depth derived from NIWA bathymetry.
Hydraulic fill	HF	Hydraulic fill (sea bed sand and mud pumped in behind retaining walls) e.g. West of Aotea Quay. SPT N<15.
Engineered fill	EF	End dumped fill and spoil materials comprised mainly of weathered basement (greywacke and argillite) and building debris.
Loose deposits	LD	Silts, clays, sands from Holocene alluvium, colluvium, beach or shallow marine deposits. SPT N < 35.
Dense deposits (upper)	DU	Interbedded sands, silts, muds and gravels from alluvium, colluvium deposits from either Holocene or Pleistocene. SPT N >35.
Dense deposits (lower)	DL	Deeper, more compacted, and therefore higher velocity unit comprised of the same lithologies as above. Set as horizontal contact at -50 m level.
*Basement surface	BS	Crushed basement sandstone, siltstone or colluvium that is sometimes referred to as "engineering basement". High velocity unit.
Greywacke basement	GB	Basement - Rakaia Terrane sandstone, siltstone and mudstone from the Torlesse Supergroup.

The Wellington and Aotea faults were modelled in 3D using surface traces extracted from the geological map and projected to the base of model using an 80° southeast dip for the Aotea Fault and an 80° northwest dip for the Wellington Fault (Figure 5.1). These fault planes controlled the boundaries between the three fault blocks. Previous 3D models of the Wellington CBD have not included the Aotea Fault. Using this structure as a fault block boundary in the model has improved our understanding of the basin structure.

The 3D geological model for this study is comprised of a basement surface with onlapping sedimentary alluvium filling the Wellington Basin that is in turn covered by recent manmade fill and sea water (Figure 5.1). The basement top contact surface was generated from surface mapping data and borehole intersections (Figure 5.2). In addition to these data, points and lines were also created in the 3D environment to constrain the basement surface where borehole or surface knowledge was limited. Examples of these include manual subsurface interpolations of depth contacts near areas of steep surface topography or valleys with sparse borehole data, as well as in the Thorndon/Centreport area where geophysical data could be used to guide the deeper basement depth in the absence of any borehole information. In the latter case, if 3D amplification effects are present the HVSR values may yield longer Tsite values than a 1D geological profile at this location with implications for bedrock depth estimates. We also cannot rule out that HVSR amplification peaks are associated with impedance contrasts between sediments and ‘rock’ material that overlies greywacke in the deepest parts of the basin; however in this case the depth to engineering bedrock is likely to be reasonable, even if the depth to greywacke basement is underestimated. Deep boreholes down to greywacke basement in the Thorndon basin would provide more clarity for the deeper sections of our model.

The dense deposits in the model were divided into two units, an upper and a lower dense deposit. The lower dense deposits (Figure 5.3) were modelled using a flat plane set at a -50 m elevation in the central CBD block and a -40 m elevation in the Mount Victoria and Tinakori Hill blocks. The upper dense deposit (Figure 5.4) top surface was modelled from borehole

contacts between these sediments and the overlying loose deposits. Loose deposits (Figure 5.5) in the model were constrained by surface mapping data and borehole contacts with younger units such as manmade fill. Surfaces for the engineered fill and hydraulic fill (Figure 5.6) surfaces were modelled from surface mapping and borehole contacts with the addition of some manually digitised lines to control the surface in regions of known fill geometry but little borehole data. The water unit was derived from NIWA bathymetry (Pallentin *et al.* 2009) elevation data. Figure 5.1–Figure 5.6 provide oblique views of each of these model surfaces as well as thickness maps of each surface.

5.2 Uncertainty Modelling

3D uncertainty modelling has been completed for this project to provide a guide of confidence at locations within the model (Figure 5.7). This uncertainty modelling uses both measures of data proximity and quality to understand the certainty we have in the 3D model at any point in the model space. Four criteria were used to create the final uncertainty value; each of these four criteria were classified using a subjective approach into a ranking scheme from one to five (one being poor certainty and 5 being high certainty).

The four criteria used to create the model were the borehole quality rank, the 3D distance to the nearest borehole, the 3D distance from a basement observation, and the 3D distance from the surface. 3D interpolation of the borehole rank score was made to create a model of the quality of the borehole logs and other records in the 3D model space (see Figure 5.7b). This identifies areas where older boreholes with poor records existed (low confidence) or where new drilling with modern logging and petrophysical techniques were used to log the borehole (high confidence). Distance to the nearest borehole trace determined by 3D distance function was used to identify areas where we have good knowledge of the subsurface or where our subsurface knowledge from borehole records is lacking (see Figure 5.7c). This geological model relies on borehole record contacts for most surfaces in the model so where there has not been drilling our confidence in the model decreases. 3D distance to the nearest observation of basement in outcrop or borehole records was used as a confidence factor because depth to basement is important when calculating 1D shear-wave velocity profiles using the model (see Figure 5.7d). Distance from the ground surface was used as a criterion as the surface is a known continuous section of data in the model (see Figure 5.7e); as distance from the ground surface increases, knowledge from boreholes and geophysical data becomes more sparse and discontinuous, reflecting a lower confidence in the data.

To assist in our understanding of the model confidence in the 3D model-space, the final uncertainty model is created from adding ranks of the four criteria within a 20 x 20 x 5 m sized model block. The most confident regions having a total result of 20 (5+5+5+5) and the least confident having a value of 4 (1+1+1+1). Figure 5.7a and Figure 5.7f illustrate the results of the uncertainty modelling in this study. The uncertainty in the model increases with depth and higher uncertainty is present in areas with poor bore hole coverage such Thorndon, the Wellington Stadium, Lambton Harbour and Frank Kitts Park areas. The model can be used to determine where data should be obtained to improve our knowledge of the subsurface and increase our confidence in the model.

5.3 Model Summary and Key Findings

This updated 3D basin model (v2.0) builds on the previous model by Semmens *et al.* (2010; v1.0) by utilising records from over 700 new boreholes, surface geological contact enhancements from LiDAR elevations, and from new 3D geological modelling techniques. The

new model interprets a shallower basement contact under the Wellington Stadium and CentrePort region; a deeper basin and possible paleochannel below Thorndon; and a fault-controlled basin west of Te Aro. The depth to basement in the current model (v2.0) is compared to the previous model (v1.0) in Figure 5.8. New interpretations of the sedimentary boundaries between loose and dense sediments and manmade fill are the result of new borehole records.

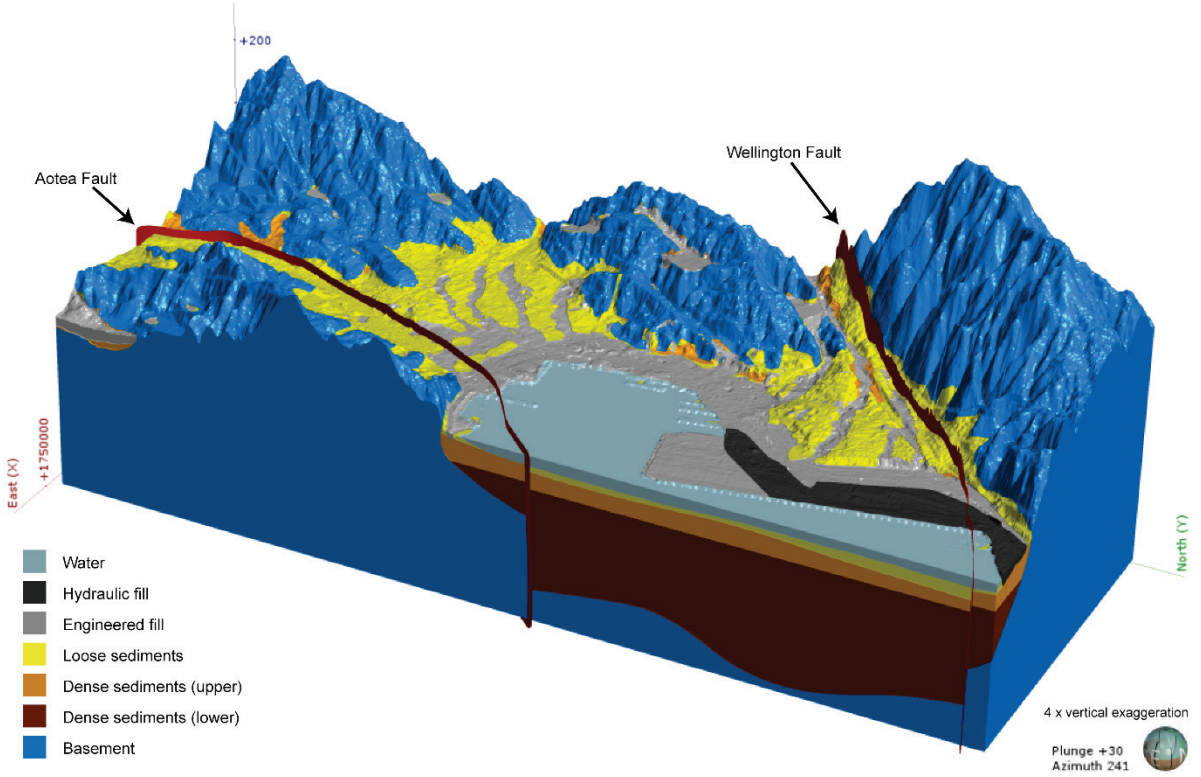

Figure 5.1 Geological model of the Wellington CBD region created from this study.

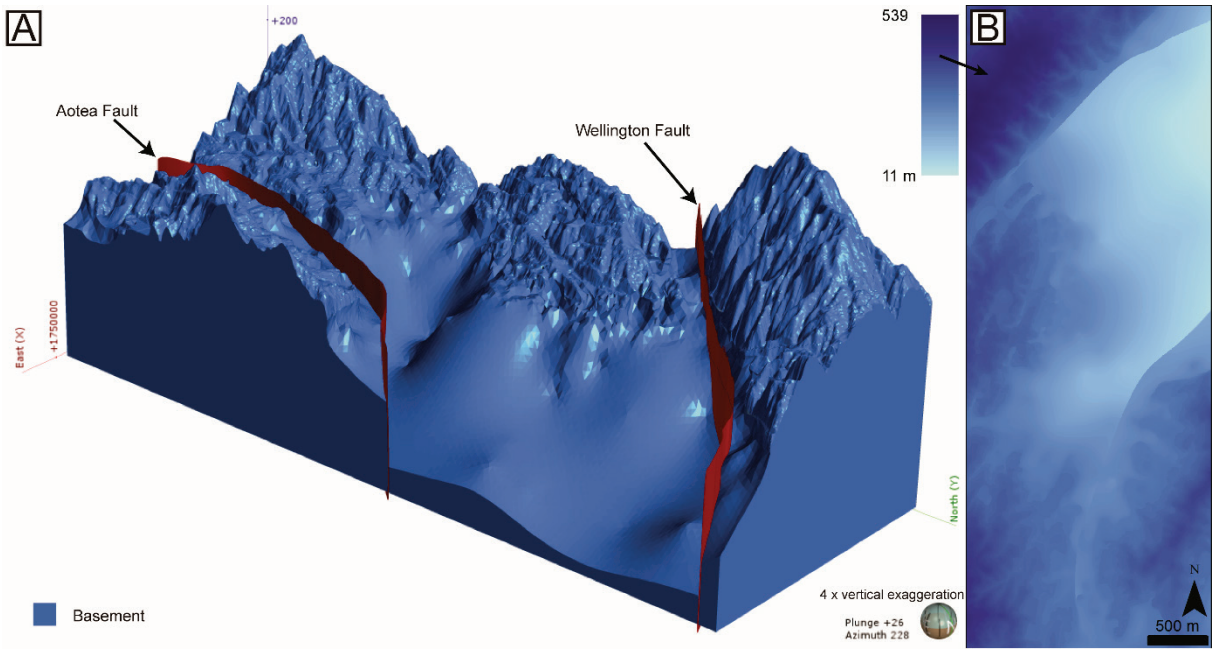

Figure 5.2 3D model and thickness calculation of basement terrane. A) Oblique view towards the SW of basement terrane and major faults; B) thickness map of basement terrain down to -250 m below sea-level.

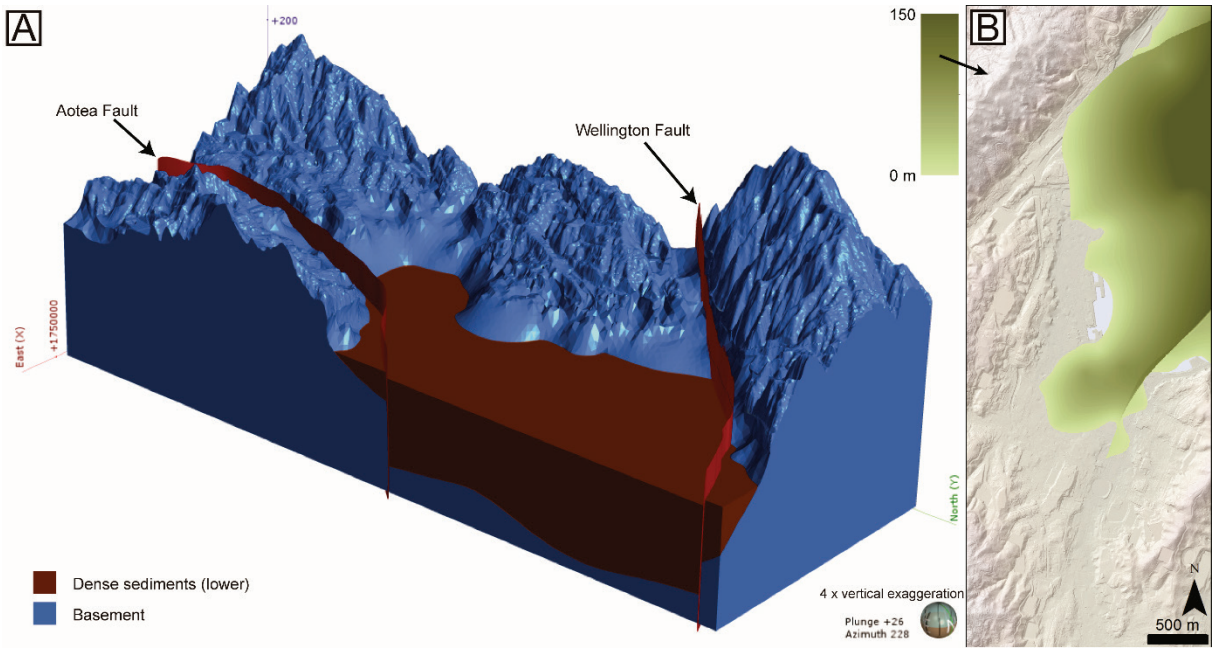

Figure 5.3 3D model and thickness calculation of lower dense sediments. A) Oblique view towards the SW of the lower dense sediments onlapping the basement terrane; B) thickness map of lower dense sediments, terrain map shown for reference.

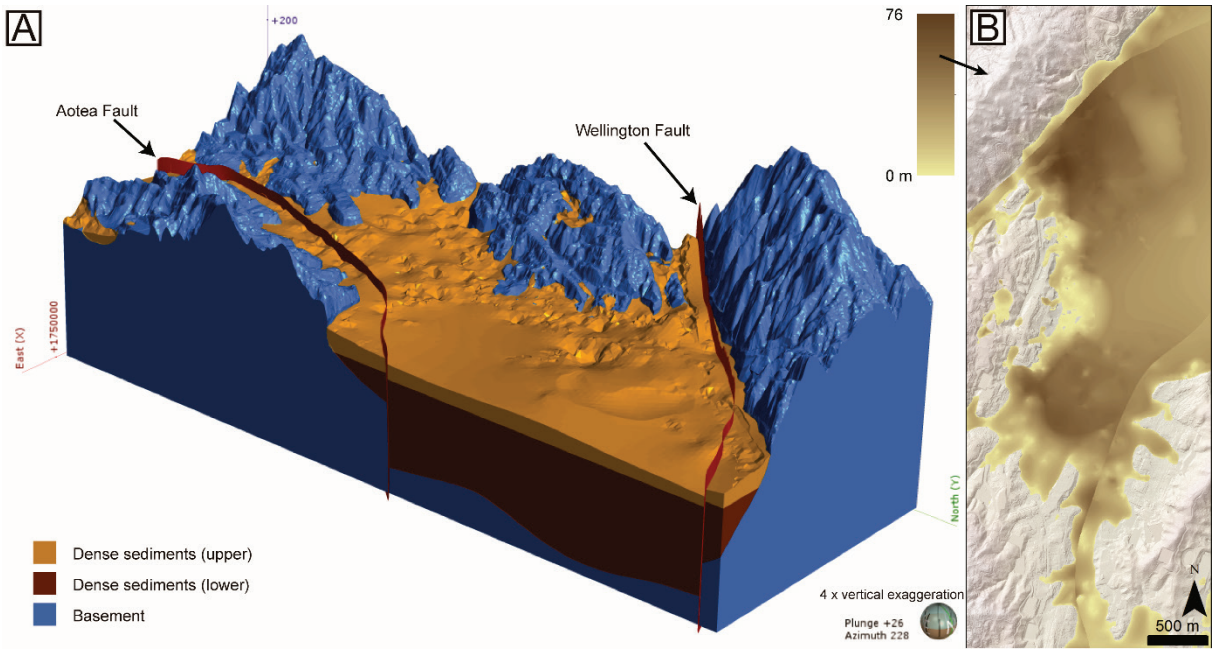

Figure 5.4 3D model and thickness calculation of upper dense sediments. A) Oblique view towards the SW of the upper dense sediments stratigraphically above the lower dense sediments; B) thickness map of upper dense sediments, terrain map shown for reference.

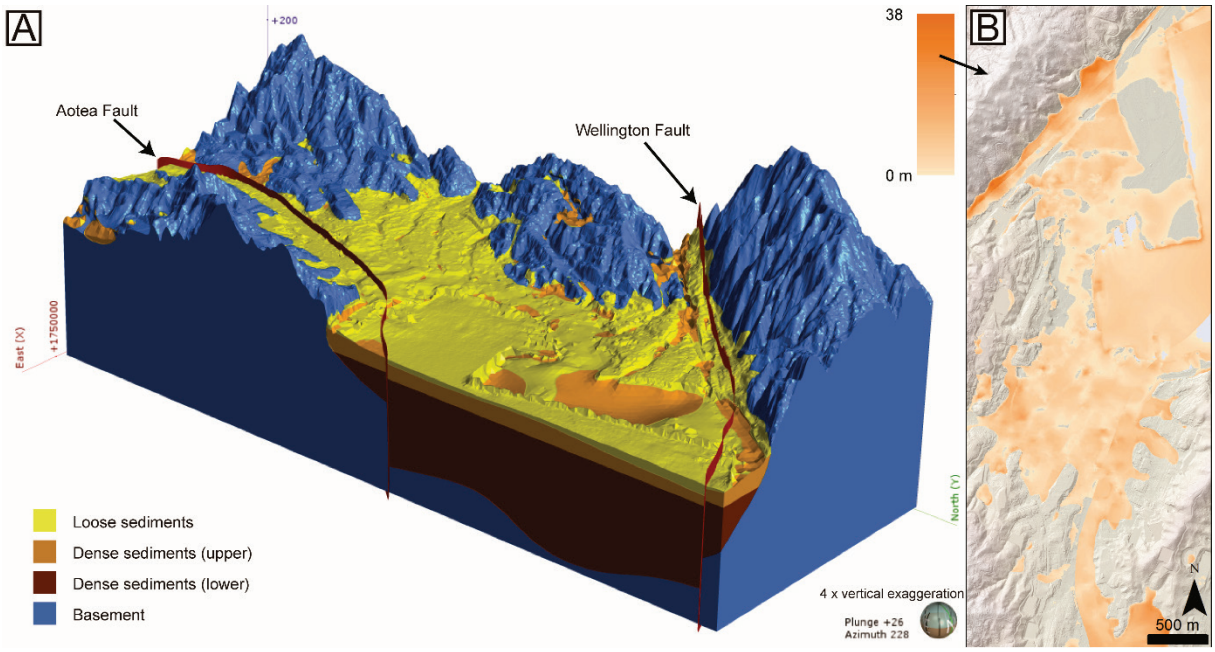

Figure 5.5 3D model and thickness calculation of loose sediments. A) Oblique view towards the SW of the loose sediments stratigraphically above the dense sediments; B) thickness map of loose sediments, terrain map shown for reference.

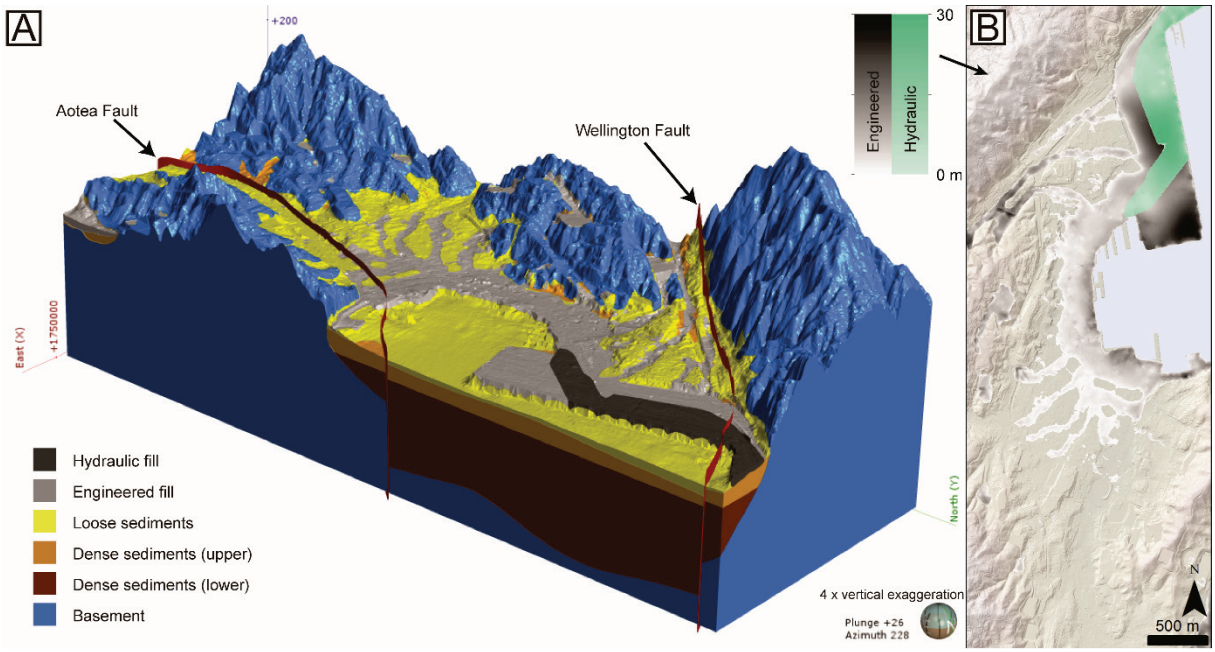

Figure 5.6 3D model and thickness calculation of man-made fill sediments. A) Oblique view towards the SW of the engineered (light grey) and hydraulic (dark grey) fill sediments; B) thickness map of the engineered (grey) and hydraulic (green) fill sediments, terrain map shown for reference.

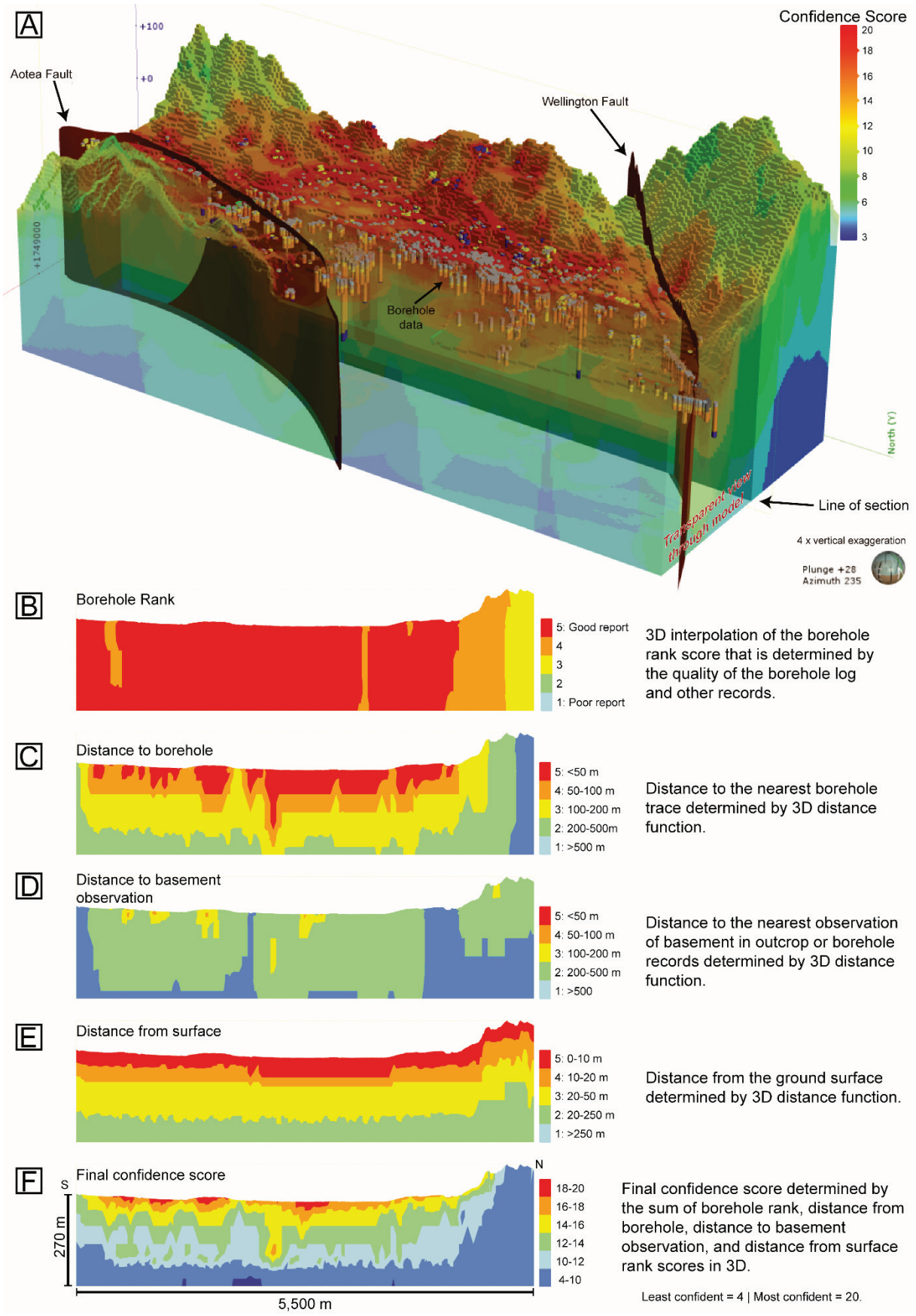

Figure 5.7 3D uncertainty model from data used in the 3D basin model (v2.0). A) oblique view of the uncertainly model showing colours representing model confidence as well as borehole locations. B-F) N-S section through the uncertainty model showing confidence data and results.

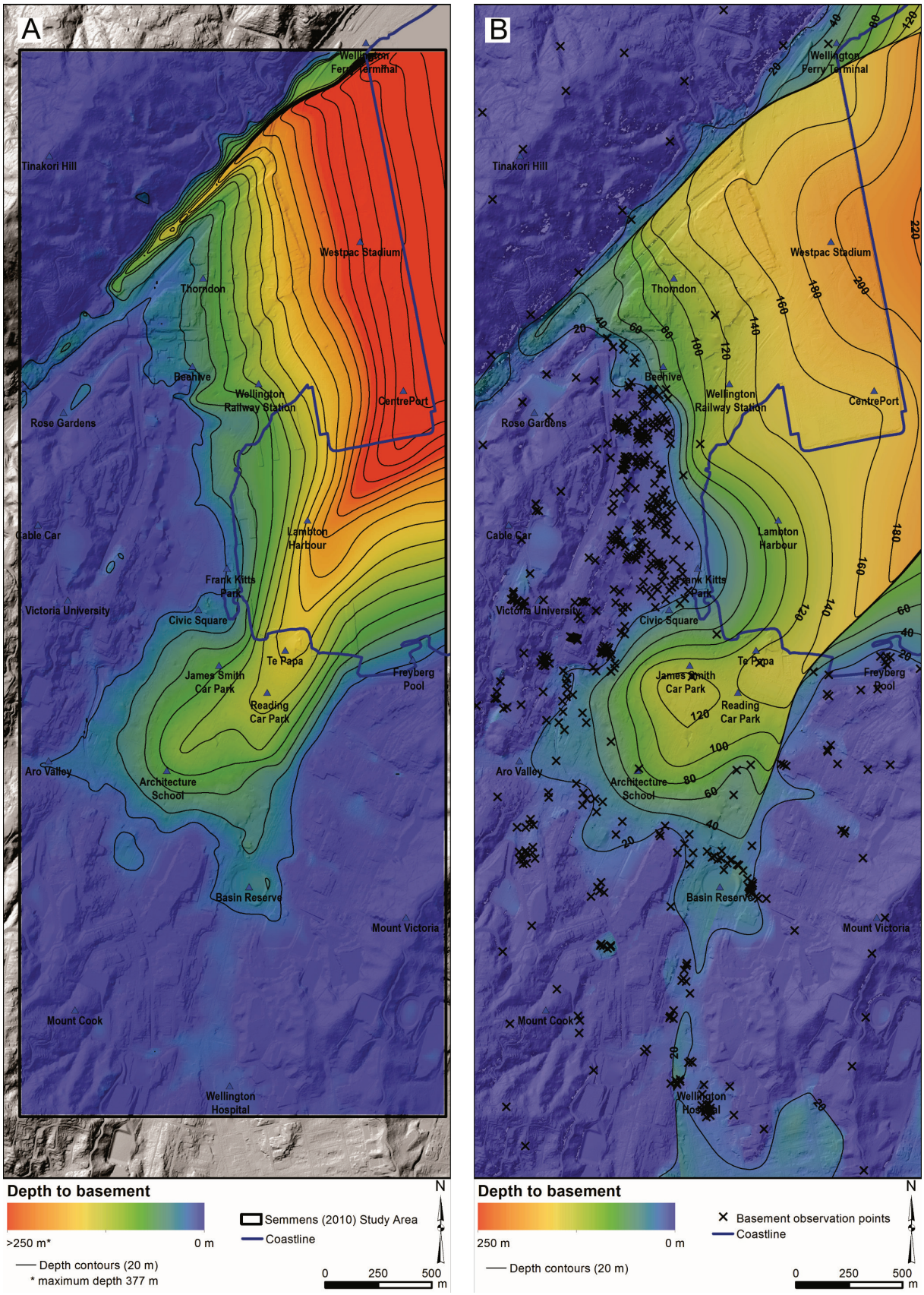

Figure 5.8 Maps of depth from the ground surface to the top basement contact derived from 3D modelling studies. A) Modelling results from Semmens (2010) in the Wellington central region — 3D basin model (v1.0). B) Modelling results from this study — 3D basin model (v2.0). 20 m interval contours plotted over colour gradient representing depth to basement, basement observation points used in the modelling also plotted for results from this study. See Appendix 1 for more details.

6.0 SITE PERIOD MAP

6.1 Map Development

We have developed a strategy to combine complementary site period information from the 3D basin model with geophysical measurements for improved mapping of site period in central Wellington (Table 6.1).

Table 6.1 Summary of key steps to develop the site period map; further details contained in the text.

Site period map development	
$Tsite_{model}$ calculated from 3D model	$Tsite_{meas}$ interpolated from geophysical measurements
Composite Tsite map compiled from steps (1) and (2) above.	
Review of mapped contours, including minor manual adjustment and smoothing.	

Firstly, site period was calculated directly from the 3D basin model based on the 1D velocity profile below the site using the FWTT approximation applied to average shear-wave velocities and thickness assigned to each engineering unit (see Table 2.1). The resulting site period distribution is shown in Figure 6.1a. Note that in this figure, sharp boundaries in site period are generated along mapped faults and geotechnical fill unit boundaries.

The 3D model site period approximation is considered to be relatively well constrained where the thickness of geological units down to basement is well-known, e.g. largely in shallow parts of the basin where boreholes-to-basement are more prevalent. In areas with both geophysical measurements and boreholes-to-basement, the site period estimates from the two approaches are generally consistent, providing validation for the velocities assigned to each engineering unit within our 3D velocity model. However, we note that the 3D model estimates are based on simple 1D assumptions and will not capture any 2D or 3D 'basin effects' that might shift the peak period of amplification, nor will they capture any spatial variations in site period due to local velocity variations within a mapped unit.

One important observation is that site period estimates from the 3D model tended to produce somewhat shorter estimated site periods than geophysical measurements at some locations where basement was known to dip steeply near the basin-edge. We infer that the geophysical measurements are capturing 2D/3D basin resonance effects, where longer period ground motions are amplified within the wider basin are also observed at the basin-edge. Furthermore, polarisation of amplification also tends to occur at these locations due to the complex subsurface topography, such that peak amplification may occur at a somewhat different period depending on the direction of motion. Given that such 3D basin effects are also present in earthquake ground motions, our study highlights the need to consider conservative approaches to site classification in such areas where 1D assumptions may be insufficient to capture the full response to earthquake shaking.

Secondly, site period was interpolated from geophysical measurements in the site period database. For this map, only measurements with a weight class of $W \geq 2$ were used (~380 total measurements), i.e. all measurements classed as 'unusable' or 'poor' were discarded. The $W \geq 2$ measurements are concentrated in the deeper parts of the Wellington basin and provide good constraints where boreholes reaching basement are sparse and the 3D model is less well-constrained. In order to integrate information across the deeper and shallower parts of the basin and reduce artefacts near the basin edges in our interpolation, we also included ~400 site period estimates extracted from the 3D model wherever boreholes reached greywacke basement and the geological profile was therefore well constrained.

The two resulting site period distributions shown in Figure 6.1 are largely compatible. Where there are differences, our analysis suggests these can largely be explained by the limitations of the underlying datasets. For example, 3D model estimates in Figure 6.1a may be inaccurate in deeper parts of the basin where layer thickness, velocity and basement depth are poorly constrained; in particular, velocity within each geotechnical unit may vary from the average velocity assigned in the 3D model. On the other hand, the 3D model produces reasonable estimates in shallow areas of the basin where site period estimates and boreholes are sparse, but sediment depth can be reasonably approximated.

Thirdly, we combine the two maps in Figure 6.1a and Figure 6.1b using a simple linear weighting scheme based on depth to basement (z):

$$Tsite = \big(1 - c(z)\big) \times Tsite_{model} + c(z) \times Tsite_{meas}$$

where if z ≤ 20 m, c = 0 (i.e. geological model estimates are adopted);

if 20 m < z ≤ 60 m, c = $\frac{(z-20)}{(60-20)}$

if z > 60 m, c = 1 (i.e. interpolated geophysical estimates are adopted) ;

The definition of parameter c was determined through trial and error to find the most reasonable result that best captures the robust features of type of data. The resulting map is shown in Figure 6.1c.

Finally, minor manual adjustments and automated smoothing were applied to accommodate any remaining problem areas which were poorly constrained in the final map. For example, smoothing of contours parallel to fault boundaries and offshore.

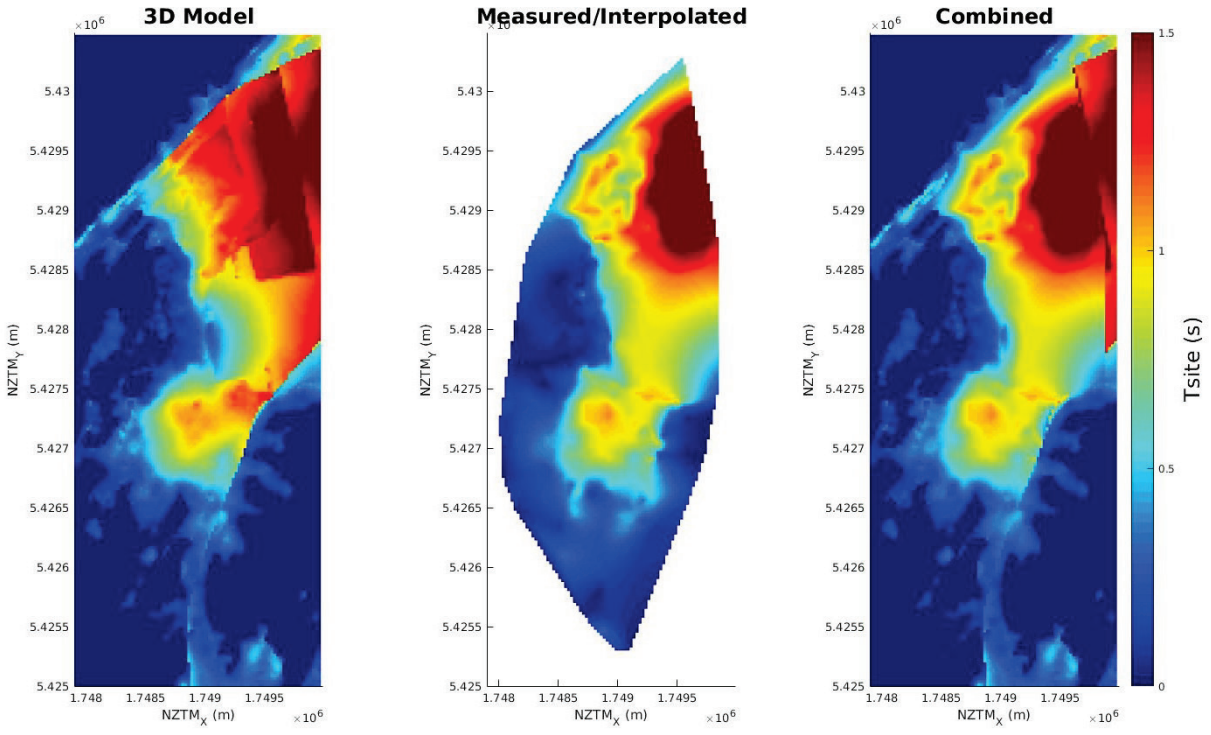

Figure 6.1 Combining information from the 3D basin model and geophysical measurements to map site period. Tsite from 3D basin model (left), interpolated geophysical measurements (middle), and combined (right) as described in Section 6.1.

6.2 Map and Key Findings

The updated site period map is shown in (Figure 6.2) along with individual site period estimates. There are some key major differences between the new site period contours and those of Semmens *et al.* (2010) illustrated in Figure 6.3.

The most significant changes occur in the Thorndon basin, which previously had only sparse measurements. The new data suggest that site period is longer than originally thought in the upper Thorndon area (e.g. between Hill St, Murphy Street and State Highway 1). This also implies that greywacke basement may be deeper than expected. In this area site period estimates are solely derived from HVSR studies and show some local variability. We infer this most likely reflects the variability of local soft soil deposits and/or basin-edge effects. It is also possible that some variations could be caused unknown 3D subsurface structures. The HVSR ratios are more complex in this area, often exhibiting two peaks (and lower 'Weight' values in our database) and this area would benefit from downhole Vs measurements to confirm basement depth and deep velocity structure.

The longest periods (>1.2 s) are largely confined to waterfront areas including reclaimed land in the Centreport area, where many high quality HVSR measurements now provide robust site period mapping. Deep Vs profiles derived from passive seismic arrays in these locations (Vantassel *et al.* 2018) are compatible with our conclusions; however, no boreholes-to-basement exist in this area, and the deeper velocity structure remains unconstrained.

The Te Aro basin site period mapping now suggests a steeper-sided, wider basin shape than that shown by Semmens *et al.* (2010). The steep eastern basin-edge is compatible with the projected location of the newly discovered Aotea Fault. Geophysical and borehole site period estimates are in excellent agreement throughout the Te Aro basin, and the deeper parts of the basin are well constrained. Furthermore, site period estimates also show smoothly varying changes across the basin which allow us to draw robust site period contours.

It is important to note that there are still large uncertainties associated with many site period estimates within ~100m of the mapped Wellington and Aotea fault traces bounding the western and eastern edges of the Wellington basin. In these areas basement depth is rapidly varying and geophysical measurements are generally of lower quality (e.g. they can be affected by complex 2D/3D effects). Furthermore, 1D assumptions inherent in the common methods to calculate site period may not adequately capture the true ground response. Additional constraints on basement depth would help to better define site period in these areas.

Our study also highlights the potentially significant influence of 2D/3D amplification effects on site response, particularly at the steep-sided basin edges. While traditional methods for determining site-period rely on estimation of the 1D soil profile, geophysical measurements of site response predict slightly longer periods of amplification in these areas.

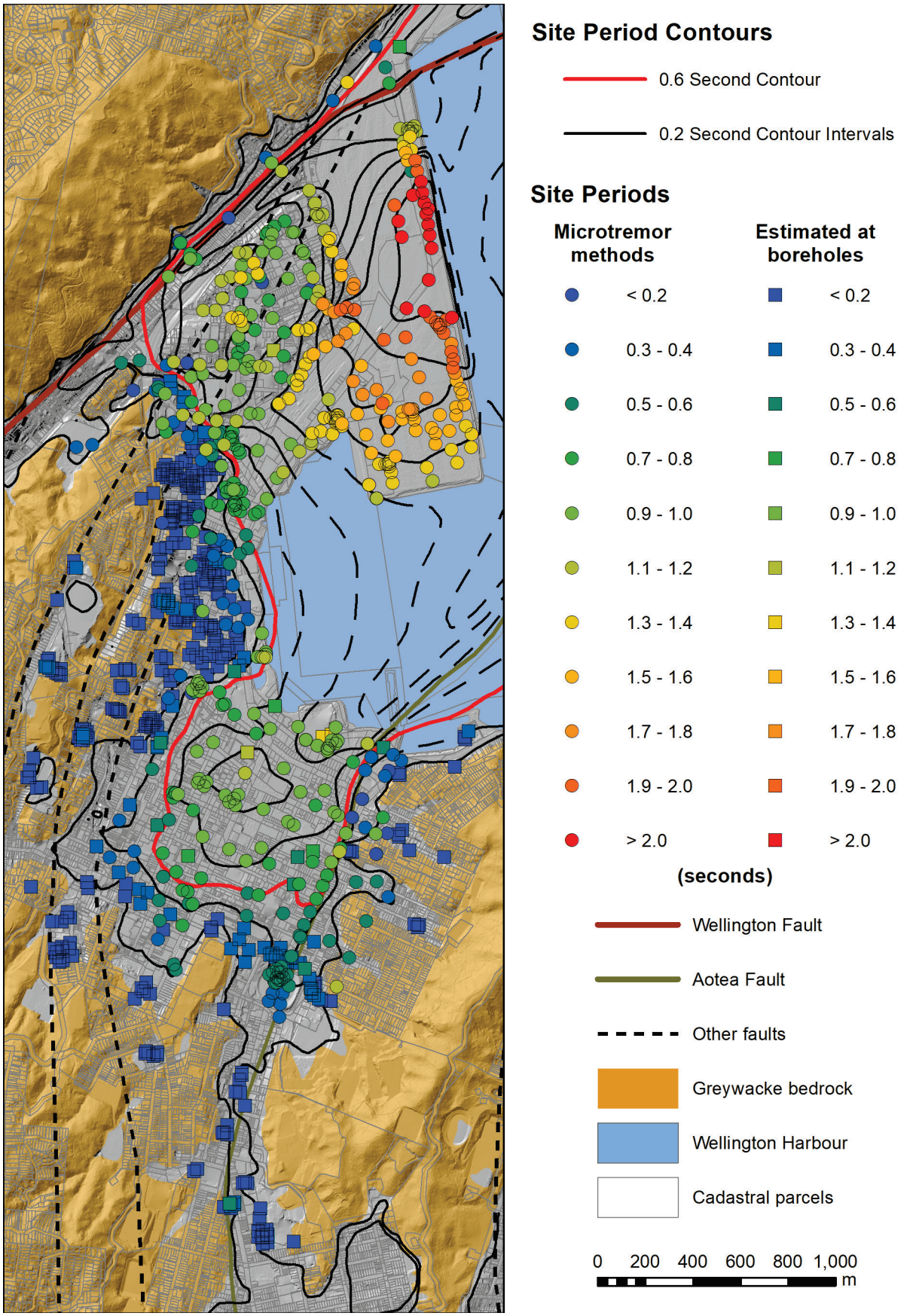

Figure 6.2 Updated site period map for central Wellington showing site period contours and locations of individual data points. See Appendix 1 for more details.

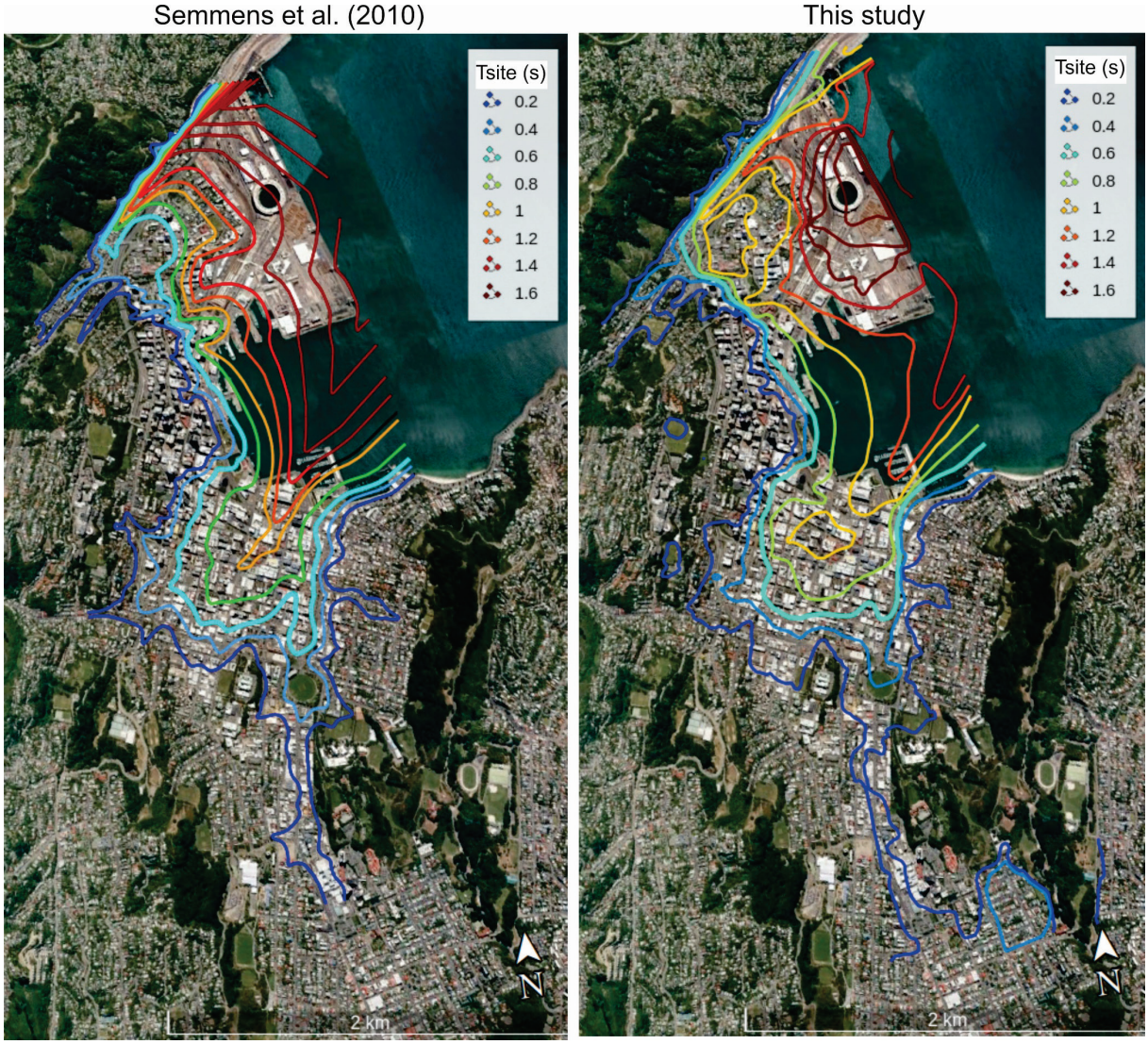

Figure 6.3 Site period contours from the previous Semmens *et al.* (2010) map compared to updated contours presented in this study.

7.0 SUBSOIL CLASS MAP

7.1 Map Development

New Zealand's NZS1170.5 loadings standard prescribes five discrete subsoil categories A–E, which are defined according to the criteria in Table 1.1 and Table 1.2. In the Wellington region, greywacke basement outcropping in the hills surrounding the basin, is designated as Class B (soft rock; e.g. Semmens *et al.* 2010). Soils within the Wellington basin range from Class C (shallow soil) – Class E (very soft soil).

In this study, we take a practical approach to block-by-block site class mapping based on the available geological and geotechnical datasets. This does not replace detailed site-specific investigation for individual building design; site-specific studies can yield additional geotechnical parameters which may allow the site classification to be refined.

Subsoil Class B/C boundary

In the Wellington region, greywacke basement outcropping in the hills surrounding the basin, is designated as Class B (e.g. Semmens *et al.* 2010). For the practical purposes of this study, we use the 3 m depth contour of the greywacke basement surface extracted from our 3D model. We consider this to be a good proxy for the class B/C boundary (see Table 1.1 NZS1170.5 Site subsoil class definitions, Standards New Zealand 2004). Given the highly variable nature of the shallow subsurface from site-to-site, we do not attempt to quantify uncertainty associated with this subsoil class boundary. However, we note that site-specific investigation can confirm basement depth, as well as yield information about degree of weathering, shear-wave velocity and/or unconfined compressive strength (UCS) which may be used to refine subsoil classification (see Table 1.1).

Subsoil Class C/D boundary

We define the Class C/D boundary based on Tsite = 0.6 s, which is consistent with the approach of Semmens *et al.* (2010) and NZS1170.5 guidelines (Standards New Zealand 2004). The mapping of the Tsite = 0.6 s contour is based on a combination of geophysical measurements and borehole data as described in detail in Section 6.0. The uncertainty of this contour is estimated by providing the site period contours equivalent to ±10% of this value.

Our approach considers that the natural site period calculated down to greywacke basement is the most appropriate site period estimate for engineering design, given that the entire soil profile contributes to ground motion amplification experienced in large earthquakes. We also note, that other definitions of the subsoil class based on soil type and its maximum depth are possible under the NZS1170.5 provisions (see Table 1.1 and Table 1.2).

Possible areas of Subsoil Class E

An area of possible Class E is outlined by the extent of hydraulic fill and observations of historical liquefaction during the Kaikōura and Cook Strait earthquakes (Cubrinovski *et al.* 2018; CS? Van Dissen?). The original intent of Class E standard was to capture liquefiable soils, which are clearly present within this area. Measurements of local shear-wave velocity (e.g. Vantassel *et al.* 2018) within this area also confirm Class E sites are present, and further investigation is underway. The extensive liquefaction observed within this outlined area highlights the need for site-specific assessment and mitigation strategies.

7.2 Map and Key Findings

New subsoil class maps show that the main features of the original Semmens *et al.* (2010) map are robust. The most significant changes to note are:

- Site period estimates for upper Thorndon consistently indicate it is most likely Class D.
- The Te Aro basin subsoil Class C/D boundary has undergone minor adjustment and is now better defined.
- Uncertainty estimates associated with the Class C/D boundary have generally been reduced, due to the large number of additional measurements.

Our updated subsoil classification maps are consistent with the 2004 NZS1170.5 standard subsoil classification guidelines. However, parallel work taking place to review NZS1170.5 spectra for Wellington subsoil classes is timely, given the advancements in seismic hazard modelling since 2004 and learnings from the Kaikōura earthquake.

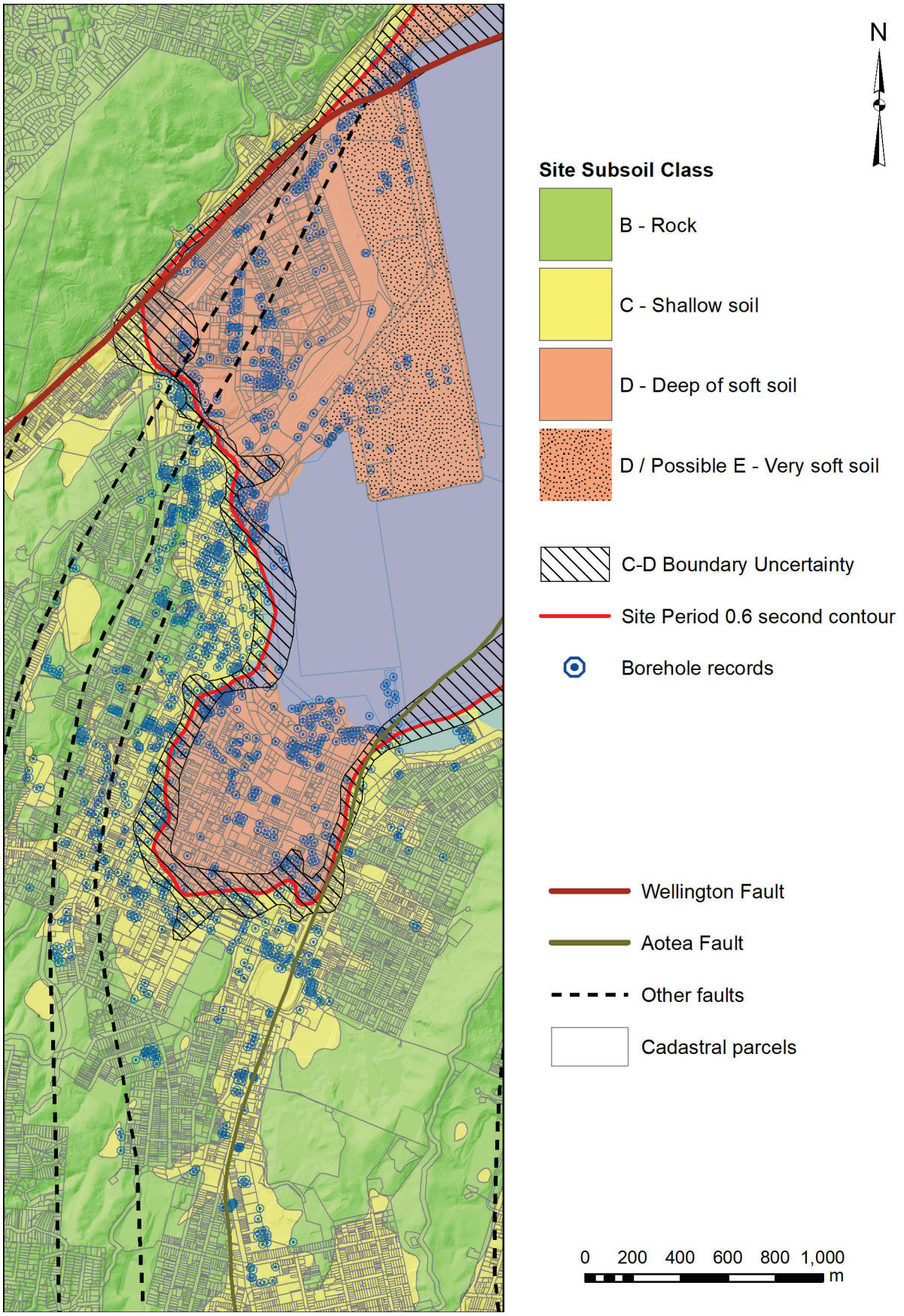

Figure 7.1 Updated site subsoil classification map for central Wellington. See Appendix 1 for more details.

8.0 DISCUSSION AND CONCLUSIONS

Following the 2016 Mw 7.8 Kaikōura earthquake, we have updated the 3D basin model and geotechnical maps for central Wellington based on significant new geotechnical data collected since the work of Semmens *et al.* (2010). The new maps and model provide additional clarity about the subsurface structure and its implications for future engineering design in Wellington.

Firstly, we have upgraded and expanded the Semmens *et al.* (2010) borehole database, which now includes 700+ additional boreholes and numerous CPT/SPT and shear-wave velocity measurements. The borehole database now comprises 1,427 boreholes, 429 of which intersect greywacke basement. We also provide an assessment of the quality of each borehole log and its geological profile in the database.

Secondly, GNS Science, the University of Auckland and collaborators from the University of Texas at Austin, have established a new geophysical site period database including over 450 site period estimates collected and collated as part of this study using the horizontal-to-vertical spectral ratio method (HVSR). The database captures details of the period, amplitude, azimuth and uncertainty associated with each measured amplification peak, as well an overall measure of quality of each site period measurement.

Thirdly, we have used the extensive new geological database to update the 3D geological basin and velocity model (v2.0) for central Wellington. Our model also includes new surface geology mapping using high resolution aerial photography and LiDAR digital terrain models. Geophysical site period estimates have been used to guide the model development in areas where the borehole database provides poor constraints. The new 3D basin geological and velocity model can be used to simulate expected ground motions and investigate 3D basin effects during large earthquakes impacting Wellington (e.g. Benites *et al.* 2005).

Finally, we draw together geological and geophysical information in an innovative scheme to provide updated maps of natural site period and site subsoil class for central Wellington. Site period is primarily constrained by available shallow boreholes reaching greywacke basement close to the basin edges, and by complementary geophysical estimates in deeper parts of the basin (i.e. depth to basement > 40 m) where deep boreholes are sparse.

The central Wellington basin is comprised of two sub-basins of greater than 100 m depth. Our results indicate that site period is longer than previously mapped in the upper Thorndon basin. This implies that the depth to greywacke basement is deeper than previously mapped in this area, and Class D is the most appropriate NZS1170.5 subsoil classification based on current evidence. Furthermore, site period estimates are variable in the Thorndon area, indicating that complex 2D/3D amplification effects associated with the Wellington Fault-bounded basin edge and/or lateral subsurface velocity variations are expected. In areas of reclaimed land, including CentrePort, site period is now much better constrained, ranging from 1.2 s to greater than 2 s. These periods correspond to the 1–2 s period range of large amplifications observed here during the Kaikōura earthquake which exacerbated damage to midrise structures (Kaiser *et al.* 2017a; Bradley *et al.* 2018).

The Te Aro basin to the south is now mapped with more steeply dipping basement on its western and eastern flanks based on our new models. In particular, the steeply dipping eastern basin edge is consistent with the projected location of the newly discovered offshore Aotea Fault (Barnes *et al.* 2018), although the precise onshore character and location of the fault trace has not been determined. If confirmed, the onshore Aotea Fault trace may have implications for land-use planning and development directly adjacent (see Kerr *et al.* 2003).

Geological and geophysical estimates of site period in the Te Aro basin are in excellent agreement and allow well-constrained mapping of smoothly varying site period contours across the basin.

One important observation from our study is the tendency of geophysical measurements at the steeply dipping basin edges to yield somewhat longer estimates of site period than predicted from 1D profiles derived from boreholes that intersect basement. In contrast, site period estimates in the centre of the basins where basement topography is flatter are generally consistent. This illustrates the need to consider the potential for 3D basin amplification effects at steeply-dipping basin-edge sites directly adjacent to deeper soil deposits; 1D boreholes at these sites may yield unconservative estimates of site period that are not able to fully capture the expected ground response.

Our 3D velocity model and maps have remaining uncertainty in two key areas where further investigation is encouraged. Depth to basement and the deeper velocity structure remains poorly constrained in the Thorndon and CentrePort area due to the lack of deep borehole data. Furthermore, basement depth (and site period) are poorly constrained directly adjacent to the Wellington and Aotea faults, where geophysical measurements are sparse and/or difficult to interpret. New deep boreholes drilled to basement would be beneficial in providing constraints on the deeper geological structure in these areas.

9.0 FUTURE DIRECTIONS AND FOLLOW-UP WORK

The updated central Wellington 3D geological and velocity model and site period map presented here will underpin future research on Wellington site and basin amplification effects. Follow-up work from this project includes:

i. Collection and collation of additional borehole-to-basement and downhole Vs data in the Thorndon and CentrePort areas to fill data gaps and better constrain bedrock depth.

ii. Review of additional shear-wave velocity information collected by GNS Science, University of Auckland, University of Texas at Austin and other Wellington consultancies since 2010. This will allow the Semmens *et al.* (2010) Vs30 map to be updated and possible refinement of the 3D velocity model.

iii. Further detailed analysis of polarization and complex 2D/3D amplification effects.

iv. Extension of our 3D basin model to link to other GNS Science 3D models covering the wider Wellington region.

v. Ground motion simulations of 3D basin amplification effects using the v2.0 3D geological and velocity model developed in this project.

10.0 ACKNOWLEDGEMENTS

This project was funded by the New Zealand Natural Hazards Platform. Supporting funds for the GNS HVSR database compilation and final report were provided by GNS SSIF. Supporting funds for the University of Auckland/University of Texas at Austin HVSR database complication were provided by QuakeCoRE, the University of Auckland EQC Capability Building Fund, and U.S. National Science Foundation (NSF) grant CMMI-1724915.

Many useful discussions and links with other research teams helped to better refine the 3D Wellington basin model. Specifically we thank the following scientists and institutions for their input: John Begg, GNS Science regarding Wellington geology; Scott Nodder, NIWA for the provision of data and advice on the Aotea Fault location; NIWA for access to Wellington harbour bathymetry data; Mark Rattenbury and Katie Jones, GNS Science, regarding 3D modelling processes; Nick Perrin, GNS Science; Aasha Pancha (Aurecon); Tracy Howe and Simon Matthews (NZGD) regarding discussion of selected borehole records and other aspects; Bill Fry regarding data interpolation techniques. We are also grateful to Chris Van Houtte and Sally Dellow for their helpful reviews of this report.

We would like to thank the New Zealand Geotechnical Database, Aurecon, Tonkin & Taylor, BECA and Coffey for access to borehole records and other subsurface data that was used in this project and improved our modelling.

Software used to generate figures and analysis for this report includes Leapfrog Geo (by Seequent), ArcGIS, Microsoft Access™, Matlab, Geopsy and Googleearth.

11.0 REFERENCES

Acerra C, Aguacil G, Anastasiadis A, Atakan K, Azzara R, Bard PY, Moreno B. 2004. Guidelines for the implementation of the H/V spectral ratio technique on ambient vibrations; measurements, processing and interpretation. [place unknown]: SAMCO. SESAME European research project, WP12 – Deliverable D23.12. European Commission – Research General Directorate Project No. EVG1-CT-2000-00026 SESAME.

Albarello D, Lunedei E. 2013. Combining horizontal ambient vibration components for H/V spectral ratio estimates. *Geophysical Journal International.* 194(2):936–951.

Anderson S, Graafhuis R, Hutchison R, Koumoutsakos D, Langdon K, Pearson K, Sisson R, Tracey B, Matthews S, McCracken S, et al. 2017. Electronic transfer of geotechnical and geoenvironmental data (AGS4 NZ v1.0.1). Wellington (NZ): New Zealand Geotechnical Society Inc.

Barnes P, Nodder S, Woelz S, Orpin A. 2014. Wellington Harbour/Te Whanganui a Tara faults. Wellington (NZ): National Institute of Water & Atmospheric Research Ltd. Client Report WLG2014–38.

Barnes PM, Nodder SD, Woelz S, Orpin AR. 2018. The structure and seismic potential of the Aotea and Evans Bay faults, Wellington, New Zealand. *New Zealand Journal of Geology and Geophysics*.62(1):46–71. doi:10.1080/00288306.2018.1520265.

Begg JG, Johnston MR. 2000. Geology of the Wellington area [map]. Lower Hutt (NZ): Institute of Geological and Nuclear Sciences. 1 folded map + 64 p., scale 1:250,000. (Institute of Geological & Nuclear Sciences 1:250,000 geological map; 10).

Begg JG, Mazengarb C. 1996. Geology of the Wellington area [map]. Lower Hutt (NZ): Institute of Geological & Nuclear Sciences. 1 map + 128 p., scale 1:50,000. (Institute of Geological & Nuclear Sciences geological map; 22).

Beetham RD, Stephenson WR, Barker PR, Perrin ND. 2010. Site classification from microtremor records, HVSR/SPAC: an effective, non-invasive site investigation method. In: Williams AL, Pinches GM, Chin CY, McMorran TJ, Massey CI, editors. *Geologically active: delegate papers 11th Congress of the International Association for Engineering Geology and the Environment;* 2010 Sep 5–10; Auckland, Aotearoa. Boca Raton (FL): CRC Press. p. 1695–1702 (paper 200).

Benites RA, Olsen KB. 2005. Modeling strong ground motion in the Wellington metropolitan area, New Zealand. *Bulletin of the Seismological Society of America.* 95(6):2180–2196.

Bradley BA, Wotherspoon LM, Kaiser AE. 2017. Ground motion and site effect observations in the Wellington region from the 2016 Mw7.8 Kaikōura, New Zealand earthquake. *Bulletin of the New Zealand Society for Earthquake Engineering*. 50(2):94–105.

Bradley BA, Wotherspoon LM, Kaiser AE, Cox BR, Jeong S. 2018. Influence of site effects on observed ground motions in the Wellington region from the Mw 7.8 Kaikoura, New Zealand, earthquake. *Bulletin of the Seismological Society of America*. 108(3B):1722–1735. doi:10.1785/0120170286.

Cubrinovski M, Bray JD, de la Torre C, Olsen M, Bradley B, Chiaro Gr, Stocks E, Wotherspoon L, Krall T. 2018. Liquefaction-induced damage and CPT characterization of the reclamations at CentrePort, Wellington. *Bulletin of the Seismological Society of America*. 108(3B):1695–1708. doi:10.1785/0120170246.

Fry B, Stephenson WR, Benites RA, Barker P. 2010. It's Our Fault: seismic instrumentation and inversion for physical parameters of Wellington and the Hutt Valley. Lower Hutt (NZ): GNS Science. Consultancy Report 2010/18.

Holden C, Kaiser AE, Van Dissen RJ,; Jury R. 2013 Sources, ground motion and structural response characteristics in Wellington of the 2013 Cook Strait earthquakes. *Bulletin of the New Zealand Society for Earthquake Engineering*. 46(4):188–195

Kaiser AE, Balfour NJ, Fry B, Holden C, Litchfield NJ, Gerstenberger MC, D'Anastasio E, Horspool NA, McVerry GH, Ristau J, et al. 2017a. The 2016 Kaikoura, New Zealand, earthquake: preliminary seismological report. *Seismological Research Letters*. 88(3):727–739. doi:10.1785/0220170018.

Kaiser AE, Van Houtte C, Perrin ND, Wotherspoon L, McVerry GH. 2017b. Site characterisation of GeoNet stations for the New Zealand Strong Motion Database. *Bulletin of the New Zealand Society for Earthquake Engineering.* 50(1):39–49.

Kerr J, Nathan S, Van Dissen RJ, Webb P, Brunsdon D, King AB. 2003. Planning for development of land, on or close to active faults: An interim guideline to assist resource management planners in New Zealand. Lower Hutt (NZ): Institute of Geological & Nuclear Sciences. 56 p. Client Report 2002/124.

Konno K, Ohmachi T. 1998. Ground-motion characteristics estimated from spectral ratio between horizontal and vertical components of microtremor. *Bulletin of the Seismological Society of America*. 88(1):228–241.

Land Information New Zealand. 2013. Wellington LiDAR 1m DEM (2013). Wellington (NZ): Land Information New Zealand.

Langridge RM, Ries WF, Litchfield NJ, Villamor P, Van Dissen RJ, Barrell DJA, Rattenbury MS, Heron DW, Haubrock S, Townsend DB, et al. 2016. The New Zealand Active Faults Database. *New Zealand Journal of Geology and Geophysics*. 59(1):86–96. doi:10.1080/00288306.2015.1112818.

McVerry GH. 2011. Site terms as continuous functions of site period and Vs30. In: *Ninth Pacific Conference on Earthquake Engineering: building an earthquake resilient society;* 2011 Apr 14-16; Auckland, New Zealand. Wellington (NZ): New Zealand Society for Earthquake Engineering. Paper 010 (8 p.).

Mortimer N, Rattenbury MS, King PR, Bland KJ, Barrell DJA, Bache F, Begg JG, Campbell HJ, Cox SC, Crampton JS, et al. 2014. High-level stratigraphic scheme for New Zealand rocks. *New Zealand Journal of Geology and Geophysics*. 57(4):402–419. doi:10.1080/00288306.2014.946062.

Nakamura Y. 1989. A method for dynamic characteristics estimation of subsurface using microtremor on the ground surface. *Quarterly Report Railway Technical Research Institute*. 30(1):25–30.

Pallentin A, Verdier A-L, Mitchell JS. 2009. Beneath the waves: Wellington Harbour. [Wellington (NZ): National Institute of Water & Atmospheric Research. (NIWA miscellaneous chart series; 87).

Semmens S. 2010. An engineering geological investigation of the seismic subsoil classes in the central Wellington commercial area [MSc thesis]. Christchurch (NZ): University of Canterbury.

Semmens S, Perrin ND, Dellow GD. 2010. It's Our Fault: geological and geotechnical characterisation of the Wellington central business district. Lower Hutt (NZ): GNS Science. Consultancy Report 2010/156.

Semmens S, Perrin ND, Dellow GD, Van Dissen RJ. 2011. NZS 1170.5:2004 site subsoil classification of Wellington City. In: *Ninth Pacific Conference on Earthquake Engineering: building an earthquake resilient society*; 2011 Apr 14–16; Auckland, New Zealand. Wellington (NZ): New Zealand Society for Earthquake Engineering.

Standards New Zealand. 2004. Structural design actions. Part 5, Earthquake actions – New Zealand. Wellington (NZ): Standards New Zealand. 82 p. (New Zealand Standard; NZS 1170.5:2004).

Standards New Zealand. 2016. Structural design actions. Part 5, Earthquake actions – New Zealand: Amendment 1. Wellington (NZ): Standards New Zealand.

Stirling MW, McVerry GH, Gerstenberger MC, Litchfield NJ, Van Dissen RJ, Berryman KR, Barnes P, Wallace LM, Villamor P, Langridge RM, et al. 2012. National seismic hazard model for New Zealand: 2010 update. *Bulletin of the Seismological Society of America*. 102(4):1514–1542. doi:10.1785/0120110170.

Strong DT, Turnbull RE, Haubrock S, Mortimer N. 2016. Petlab: New Zealand's national rock catalogue and geoanalytical database. *New Zealand Journal of Geology and Geophysics*. 59(3):475–481. doi:10.1080/00288306.2016.1157086.

Van Dissen RJ, McSaveney MJ, Townsend DB, Hancox GT, Little TA, Ries W, Perrin ND, Archibald GC, Dellow GD, Massey CI, et al. 2013. Landslides and liquefaction generated by the Cook Strait and Lake Grassmere earthquakes: a reconnaissance report. *Bulletin of the New Zealand Society for Earthquake Engineering*. 46(4):196–200.

Vantassel J, Cox B, Wotherspoon L, Stolte A. 2018. Mapping depth to bedrock, shear stiffness, and fundamental site period at CentrePort, Wellington, using surface-wave methods: Implications for local seismic site amplification. *Bulletin of the Sesimological Society of America.* 108(3B):1709–1721.

Wood RA, Davy BW. 1992. Interpretation of geophysical data collected in Wellington Harbour. Lower Hutt (NZ): Institute of Geological & Nuclear Sciences. Client Report 1992/78.

APPENDICES

This page left intentionally blank.

APPENDIX 1 A3 MAPS

Map 1: Depth to Bedrock

Map 2: Natural Site Period

Map 3: NZS1170.5:2004 Site Subsoil Class

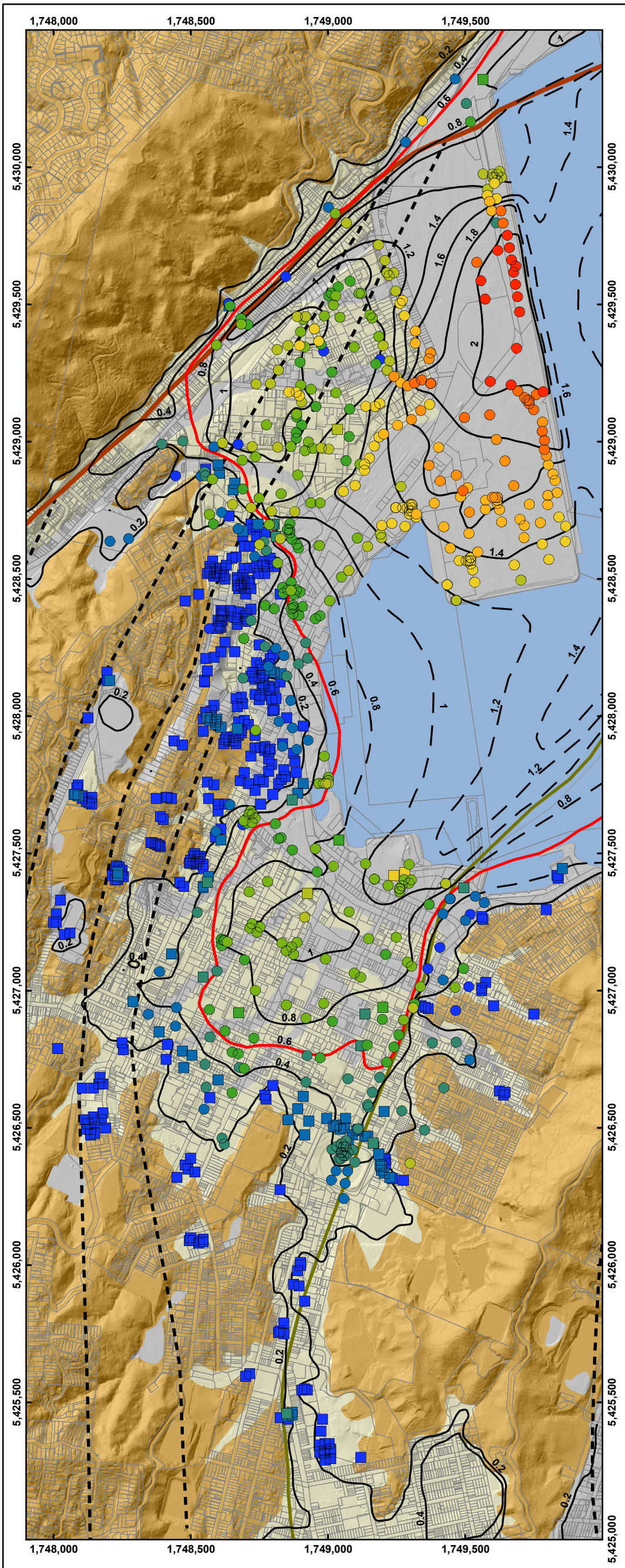

N

Central Wellington Low Amplitude Natural Period (V2.0)

Map shows low amplitude natural period contours over 0.2 second intervals for the Wellington central business district, updated from Semmens et al. (2010). This map has been constructed using available measured and modelled site period information (refer to accompanying report for details). Note, that no subsurface information was available for the harbour area and the contours in this area (shown as dashed lines on map) have a low confidence.

Legend

Site Period Contours

- 0.6 Second Contour
- 0.2 Second Contour Intervals

Site Periods

Microtremor methods	Estimated at boreholes
< 0.2	< 0.2
0.3 - 0.4	0.3 - 0.4
0.5 - 0.6	0.5 - 0.6
0.7 - 0.8	0.7 - 0.8
0.9 - 1.0	0.9 - 1.0
1.1 - 1.2	1.1 - 1.2
1.3 - 1.4	1.3 - 1.4
1.5 - 1.6	1.5 - 1.6
1.7 - 1.8	1.7 - 1.8
1.9 - 2.0	1.9 - 2.0
> 2.0	> 2.0

(seconds)

- Wellington Fault
- Aotea Fault
- Other faults
- Wellington Harbour
- Fill
- Quaternary sediments
- Greywacke bedrock
- Cadastral parcels

This map provides a starting point for geotechnical investigations, but does not replace the need for professional consultation and site specific investigations.

0 200 400 600 800 1,000 m

PROJECTION: NZGD 2000 New Zealand Transverse Mercator

REFERENCE:

Kaiser, A.E.; Hill, M.P.; Wotherspoon, L.; Bourguignon, S.; Bruce, Z.R.; Morgenstern, R.; Giallini, S. 2018. Updated 3D basin model and NZS 1170.5 subsoil class and site period maps for the Wellington CBD: Project 2017-GNS-03-NHRP. GNS Science consultancy report 2019/01.

Digital terrain model and cadastral parcels from LINZ; faults from Heron (2018) and Langridge et al. (2016).

DRW: MH

CHK: AK

GNS SCIENCE TE PŪ AO

Map 1
Low Amplitude Natural Period
V2.0

Wellington City
New Zealand

Appendix 1

Map 1

REPORT: GNS CR 2019/01

DATE: March 2019

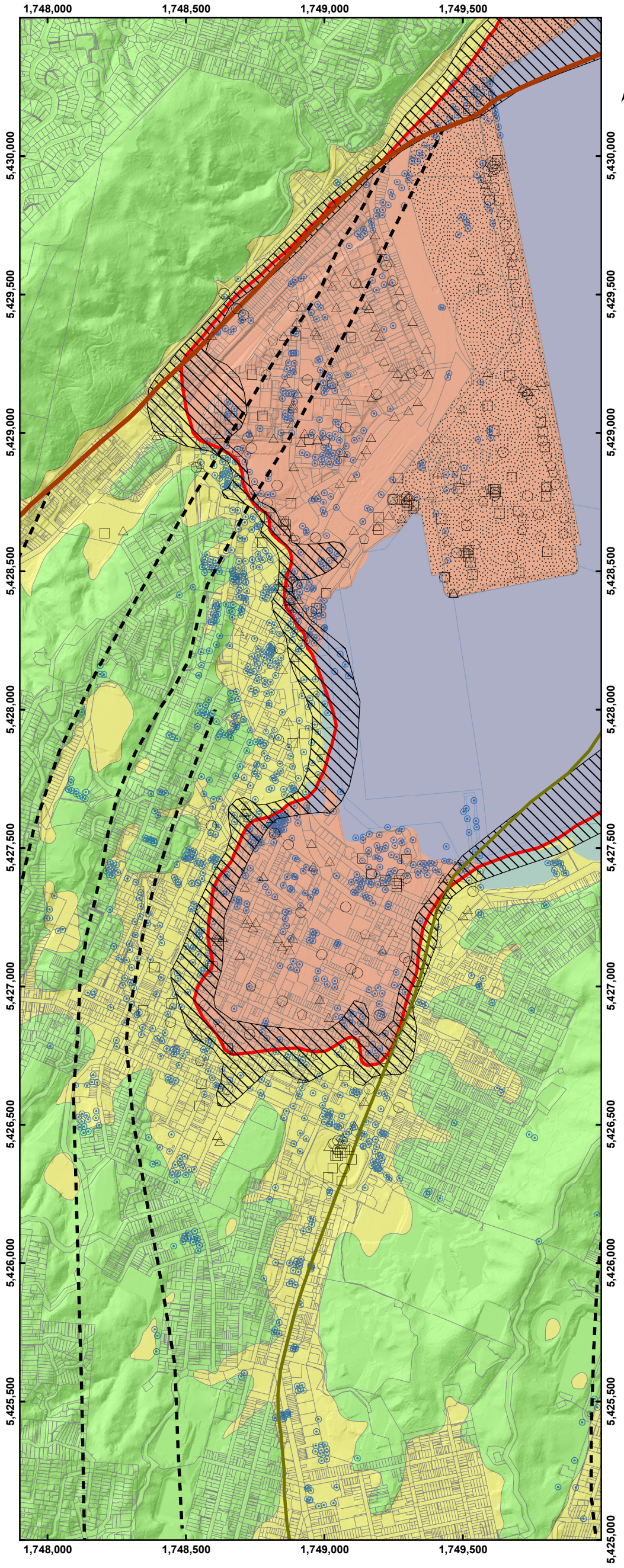

N

Central Wellington NZS1170.5:2004 Site Subsoil Class (V2.0)

Map shows NZS1170.5:2004 site subsoil classes for central Wellington based on the specific criteria outlined below extracted from NZS1170.5:2004 guidelines. Note, that in this study, the mapped class B/C and class C/D boundaries are based on the modelled depth of surface layer and low amplitude natural site period respectively. The full NZS1170.5 site subsoil class criteria allow for site-specific interpretations incorporating additional data types not fully considered here. Uncertainty in the subsoil class B/C boundary is not evaluated and uncertainty in the C/D boundary is illustrated by the hatched area. The dotted area contains possible Class E soils based on the analysis of Semmens et al. (2010) and historical observations of liquefaction (see details in text).

Legend

- Borehole records
- Site Period 0.6 second contour
- C-D Boundary Uncertainty

Site Subsoil Class	Definition used specifically in this study Full definitions and criteria for each subsoil class can be found in Standards NZ 2004.
B Rock	A surface layer (completely to highly weathered rock/soil) no more than 3m depth, as defined by geological model.
C Shallow Soil	Low amplitude natural period ≤ 0.6 s as defined by new site period map compiled in this study and not Class B.
D Deep or Soft Soil	Low amplitude natural period > 0.6 s as defined by new site period map compiled in this study.
D / Possible E Deep or Soft Soil / Possible Very Soft Soil	Area currently under detailed investigation and may contain Class E sites. Hydraulic Fill is found within this area and historical liquefaction was observed within this area during the 2016 Kaikoura earthquake and 2013 Cook Strait earthquakes.

- Wellington Fault
- Aotea Fault
- Other faults
- Cadastral parcels

Site Period Sites (data rank)

- 5
- 4
- 3
- 2

This map provides a starting point for geotechnical investigations, but does not replace the need for professional consultation and site specific investigations.

0 200 400 600 800 1,000 m

PROJECTION: NZGD 2000 New Zealand Transverse Mercator

REFERENCE:

Kaiser, A.E.; Hill, M.P.; Wotherspoon, L.; Bourguignon, S.; Bruce, Z.R.; Morgenstern, R.; Giallini, S. 2018. Updated 3D basin model and NZS 1170.5 subsoil class and site period maps for the Wellington CBD: Project 2017-GNS-03-NHRP. GNS Science consultancy report 2019/01.

Digital terrain model and cadastral parcels from LINZ; faults from Heron (2018) and Langridge et al. (2016).

DRW: MH

CHK: AK

GNS SCIENCE TE PŪ AO

Map 2
Central Wellington NZS1170.5:2004 Site Subsoil Class (V2.0)

Wellington City New Zealand

Appendix 2

Map 1

REPORT: GNS CR 2019/01

DATE: March 2019

Central Wellington Depth to Basement from 3D Geological Model (V2.0)

Map shows the depth to the Rakaia Terrane basement from the topographic surface. The map has been generated from an exported surface from the 3D geological model that was created using borehole intersections, geophysical data, surface observations and geological mapping. These depths can be considered as a proxy for Z1.0 (depth to 1 km/s material) for Wellington.

Legend

- Open file borehole records with basement intersection
- Depth to basement contours (20 m)
- Coastline

Depth to basement

200 m — 0 m

- Wellington Fault
- Aotea Fault
- Other faults
- Cadastral parcels

This map provides a starting point for geotechnical investigations, but does not replace the need for professional consultation and site specific investigations.

0 200 400 600 800 1,000 m

PROJECTION: NZGD 2000 New Zealand Transverse Mercator

REFERENCE:

Kaiser, A.E.; Hill, M.P.; Wotherspoon, L.; Bourguignon, S.; Bruce, Z.R.; Morgenstern, R.; Giallini, S. 2018. Updated 3D basin model and NZS 1170.5 subsoil class and site period maps for the Wellington CBD: Project 2017-GNS-03-NHRP. GNS Science consultancy report 2019/01.

Digital terrain model and cadastral parcels from LINZ; faults from Heron (2018) and Langridge et al. (2016).

DRW: MH

CHK: AK

Map 3 Central Wellington Depth to Basement from 3D Geological Model (V2.0)

Wellington City New Zealand

Appendix 3

Map 1

REPORT: GNS CR 2019/01

DATE: March 2019